Protocol
for the Quality Control of the Physical and Technical Aspects of Digital Breast Tomosynthesis Systems

version 1.0

March 2015

Authors:

R.E. van Engen, Nijmegen, the Netherlands (Corresponding author)*
H. Bosmans, Leuven, Belgium*
R.W. Bouwman, Nijmegen, the Netherlands
D. R. Dance, Guildford, United Kingdom
P. Heid, Marseille, France*
B. Lazzari, Pistoia, Italy*
N. Marshall, Leuven, Belgium
S. Schopphoven, Marburg, Germany*
C. Strudley, Guildford, United Kingdom
M.A.O. Thijssen, Arnhem, the Netherlands*
K.C. Young, Guildford, United Kingdom*

* Members of Physico-technical Steering Group

Contributors:
J. Binst, Leuven, Belgium
K. Lemmens, Leuven, Belgium
A. MacKenzie, Guildford, UK
S. Menhart, Vienna, Austria
J. Oduko, Guildford, UK
V. Ravaglia, Lucca, Italy
F. Semturs, Vienna, Austria
W. Veldkamp, Leiden/Nijmegen, the Netherlands
R. Visser, Deventer, the Netherlands

Corresponding author:
R. van Engen
R.vanEngen@lrcb.nl
Dutch reference centre for screening
P.O. Box 6873
6503 GJ Nijmegen
The Netherlands

Collaborating institutes:

Individual meetings at ECR 2013 were held with and comments were received from:
Barco, General Electric, Philips, Hologic, IMS, Siemens

Participants at ECR 2013 and 2014 meetings:

S. Avramova-Cholakova, Bulgaria
H. Bosmans, Leuven, Belgium
D. Bödeker, IBA dosimetry
R.Bouwman, Nijmegen, the Netherlands
A. Carvalho, Gamma-X
T. Chouliaras, Sweden
F. Cirillo, Metaltronica
G. Dobrozemsky, Austria
A. Dolińska, Poland
O. Dragusin, Luxemburg
S.E. Ehlers, Germany
E. Fabiszewska, Poland
S. Flatabø, Norway
E. Gabriel, Austria
G. Gennaro, Italy
L. Gobbi, Italy
P. Heid, Marseille, France
B. Hemdal, Sweden
H. de las Heras, Quart
A. van Hulzen, the Netherlands
M. Hörnig, Siemens
W. Hummel, the Netherlands
B. Ibi, Austria
M. Kaar, Austria
A. Kamandzenka, Adani
R. Klausz, General Electric
A. Kuchcińska, Poland
M. Leung, IBA dosimetry
J. Lindström, Sweden
R. Magauer, Austria
F. Malchair, Belgium
B. Martins, Hologic
N. Marshall, Leuven, Belgium
J. McCullagh, Ireland
S. Menhart, Austria
T. Mróz, Poland
J. Müller, Fujifilm Europe
L. Niklason, Hologic
A. Noel, France
N. Oberhofer, Italy
M. Ogoda, Fujifilm Europe
M. Olejnik, Poland
A. Osanna Elliot, Austria
K. Pasicz, Poland
E. Pater, Poland
K. Pedersen, Norway
J. Rosenitsch, Austria
J. Scherp Nilsson, Sweden
S. Schopphoven, Marburg, Germany
I. Schulze-Wenck, Philips
I. Sechopoulos, USA
F. Semturs, Austria
T. Sendai, Fujifilm Japan
A. Smith, Hologic
T. Sobczak, Germany
A. Sommer, Germany
A. Stembert, Belgium
M. Szewczyk, Poland
E. Sturm, Austria
S. Thunberg, Sweden
P. Torbica, Austria
J. Trupp, IBA dosimetry
R. van Engen, Nijmegen, the Netherlands
S. Vecchio, IMS
M. Verius, Austria
B. Wendt, Germany
M. Weżgowiec, Poland
S. Wildner, Austria
A. Xthona, Barco
K. Young, Guildford, United Kingdom
G. Zwettler, Austria

Additional comments have been received from the following members of the American Association of Medical Physicists tomosynthesis subcomittee:
K. Chakrabarti FDA, USA
B. Lui, USA
M. Goodsitt, USA

On september 17, 2014 a common meeting with the International Electrotechnical Committee MT 31 has been held.

Contents

Introduction

The fourth edition of the European Guidelines for breast cancer screening and diagnosis, and its supplement, have been used as a starting point for the development of this protocol (Perry et al 2006, Perry et al 2013). This protocol is work-in-progress and should be regarded as a preliminary protocol for quality control in Digital Breast Tomosynthesis (DBT). Large parts of the protocol are supported by scientific research (van Engen 2008, Marshall 2010, Bouwman 2010, Jacobs 2010, Dance 2011, Bouwman 2012, Marshall 2012, Bouwman 2013).

Scope:

This protocol applies only to tomosynthesis systems which measure X-ray transmission through the breast over a limited range of angles, followed by reconstruction of a series of images of the breast reconstructed for different heights above the detector. These images represent breast tissue at the height of the corresponding focal planes as well as a remaining portion of overlying tissue. In this protocol such systems will be referred to as DBT systems. This imaging modality is distinct from computed tomography (CT) in which a three dimensional image is reconstructed using X-ray transmission data from a rotation of at least 180º around the imaged volume (Dobbins 2009, Sechopoulos 2013).

This protocol does not apply to CT or any other mammographic modalities such as conventional 2D imaging, stereotactic imaging using pairs of images, or any other form of reconstructive tomography.

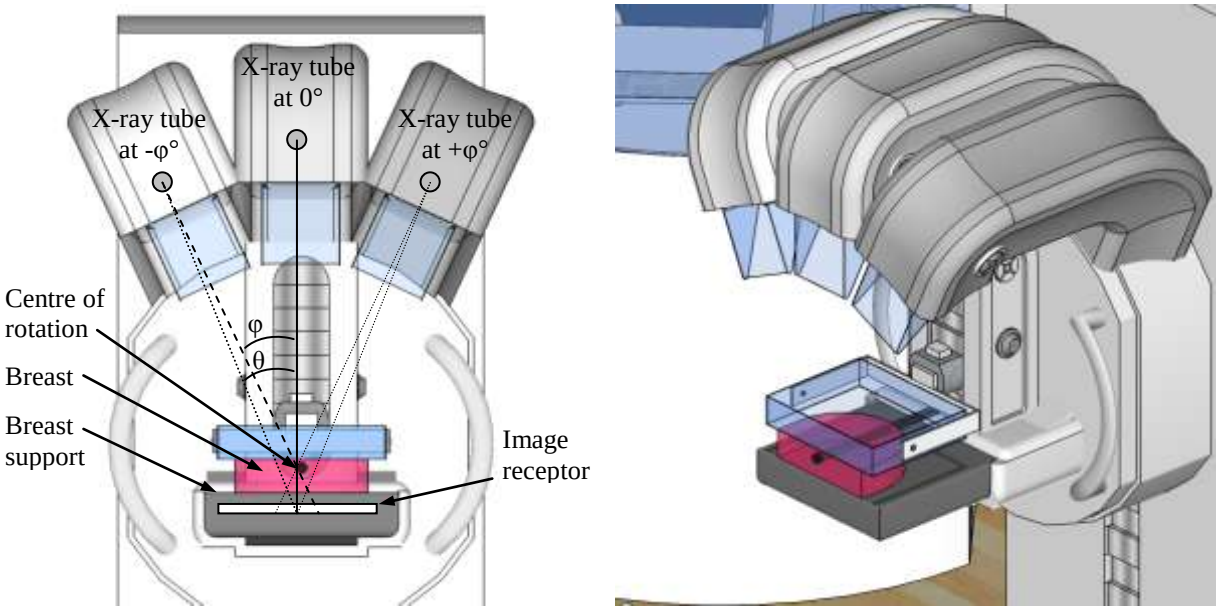

Figure 1 Typical geometry used for a breast tomosynthesis system with a full field detector, showing three positions of the X-ray tube, the tube rotation angle φ and the projection angle θ for the rotated position (not to scale).

Two types of DBT geometries are currently available or under development:

1. Full-field geometry: DBT systems incorporating a detector, as used in conventional 2D full field digital mammography (FFDM), and an X-ray tube that rotates above this detector. A series

of individual projection images, in which the whole breast is irradiated in each exposure, is acquired over a range of angles, as shown in Figure 1.

2. Scanning geometry: Geometry of DBT systems utilising a narrow collimated X-ray beam which scans across the breast as the X-ray tube rotates, and by which the breast is only partially irradiated at each position of the X-ray tube. Due to the design of the system, individual projection images might not exist.

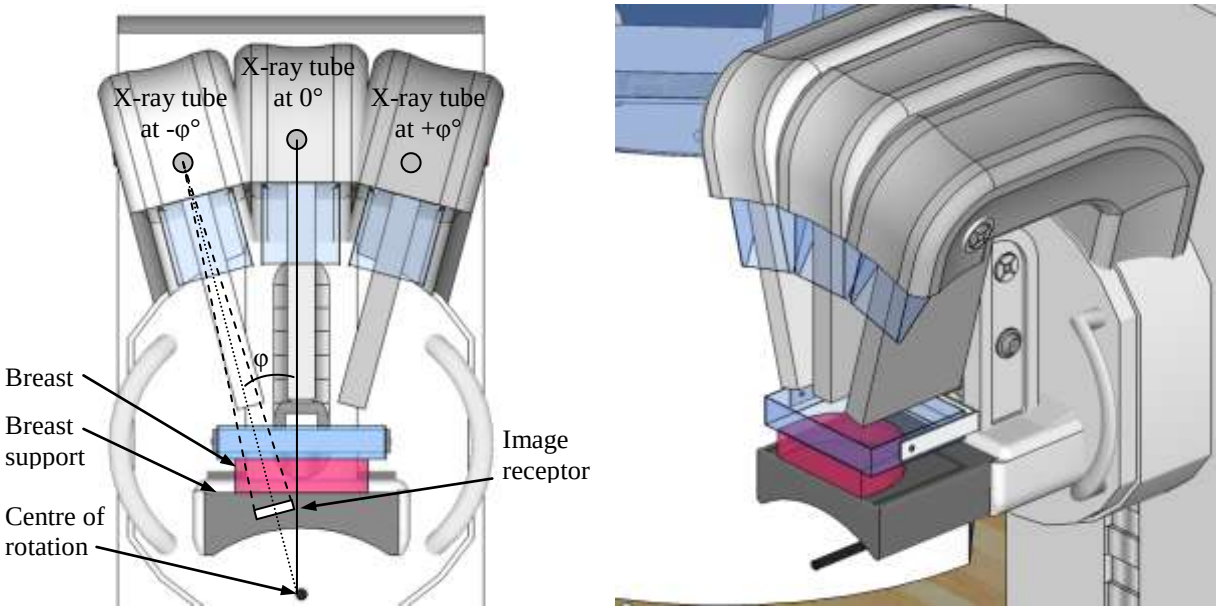

Figure 2 Geometry of a scanning breast tomosynthesis system with a narrow X-ray beam (currently under development) showing three positions of the X-ray tube (not to scale). In this system both the X-ray tube and image receptor rotate. The X-ray field is collimated to the image receptor. The limits of the X-ray field and the ray passing through the centre of rotation are shown.

In Table 1 specifications and geometry of currently available or prototype DBT systems can be found. These geometries have been taken into account for the calculation of the dosimetry factors (T-factors) in appendix I.

In FFDM the signal from the detector forms an 'original data' image, to which corrections are applied, including a flat-field correction for 'bad' (or defective) pixels and for non-uniformities of the radiation field, corrections for the offset and gain of detector elements, geometrical distortion and for readout time variation. This corrected image is referred to as the 'for processing' or unprocessed image. The unprocessed image is then processed to adjust the appearance of clinical images, resulting in the 'for presentation' or processed image.

In DBT the signals of the individual DBT projection images from the detector are corrected for bad pixels and non-uniformities of the radiation field, offset and gain of detector elements, geometrical distortion and time variation during a scan. The corrected projection images may then be pre-processed before they are used for the reconstruction. After reconstruction, mammography specific post-processing may be applied. Alternatively, some of the mammography specific processing may be incorporated into the image reconstruction process.

In several tests in the present protocol, we refer to the 'first projection image of a DBT series'. This projection image will not be influenced by lag from previous exposures of the DBT series. If for whatever reason, the first image is different from the subsequent series, the second image should be used instead. Examples include the first projection being used for automatic exposure control or for another calibration purpose.

Table 1 Specifications and geometry of breast tomosynthesis systems currently available or in development (based on Sechopoulos 2013 and subsequent information from manufacturers).

DBT System	*General Electric SenoClair*	*Hologic Selenia Dimensions*	*IMS Giotto TOMO*	*Philips Microdose*	*Planmed Clarity3D*	*Siemens Mammomat Inspiration*	*Fujifilm Amulet Innovality*
Type of geometry	Full-field	Full-field	Full-field	Scanning multislit	Full-field	Full-field	Full-field
Detector type	Energy integrating	Energy integrating	Energy integrating	Photon counting	Energy integrating	Energy integrating	Energy integrating
Detector material	CsI-Si	a-Se	a-Se	Si	CsI-a-Si	a-Se	a-Se
Detector element size (µm)	100	70	85	50	83	85	68[5]
Focal plane pixel size (µm)	100	95-117[1]	90	100	83/166	85	100/150
X-ray tube motion	Step-and shoot	Continuous	Step-and shoot	Continuous	Continuous, Sync-and-Shoot	Continuous	Continuous
Target	Mo/Rh	W	W	W	W	W	W
Filter	Mo: 30µm Rh: 25 µm	Al: 700 µm	Rh: 50 µm Ag: 50 µm	Al: 500 µm	Rh: 75 µm Ag: 60 µm	Rh: 50 µm	Al: 700 µm
Angular range	25	15	40[2]	N/A[6]	30	50	15/40
Number of projection images	9	15	13	21[3]	15	25	15
Source to detector distance (mm)	660	700	685	660	650	655	650
Distance between detector and centre of rotation (mm)	40	0	20	400[4]	4.4	47	46

[1] The pixel size in the focal plane changes with height above the breast support table.
[2] The projection images may not be equally spaced and may not have the same exposure factor.
[3] This system does not have projection images, but 21 datasets from the detector lines.
[4] Below the detector.
[5] Hexagonal shaped detector elements.
[6] Tube movement: 34°.

Aim of this draft version:

DBT systems are currently available on the market and the number of installations rapidly increases. DBT systems are also considered for breast cancer screening. Guidance on Quality Control (QC) measurements for these systems is necessary and therefore it has been decided that this protocol should be made available in its present phase even though it does not yet cover all aspects of DBT performance testing and incorporates some QC tests which are not in their final version. The tests described in this protocol can be used to characterize DBT systems, to test their stability and to perform dose measurements. In most cases, limiting values are not yet given; more experience with DBT, results of clinical trials and /or technical performance tests are necessary to determine the limiting technical requirements. In this document, reference values are given in several cases which have been derived from full field digital mammography (FFDM).

We emphasise that dose limiting values from FFDM should not be used as limiting values for DBT systems, but should be used as reference values. Another reason for distributing this protocol at an early stage is that physicists may need specific imaging modes to facilitate adequate testing. A main objective of this document is to ensure that access to these imaging modes is made available.

This protocol does not give any advice or guarantee on the suitability of DBT equipment for any particular clinical task.

Some DBT systems are able to perform both FFDM and DBT imaging, and some DBT systems are capable of synthesizing a 2D image from the DBT data set. The FFDM modality should be tested according to the current version of the European Guidelines (van Engen 2006) and its Supplement (van Engen 2013). This protocol focuses on the DBT modality and does not give guidance on synthesized 2D images.

The test methods described are intended to be applicable to all currently available DBT systems. However, the differences between the full-field DBT systems currently available and in development, and the scanning geometry systems in development are such that some QC tests have to be adjusted to be used for these geometries. The development of the DBT QC tests started with an evaluation of whether existing FFDM QC tests could be adapted for use with DBT systems. This approach was appropriate because most current DBT systems are based on existing FFDM systems. Different system design and implementations occur, for example, in the movement of the X-ray tube and/or the detector, the use of an anti-scatter grid, beam quality and the detector readout sequences. While radiographic images are ‘processed’ for presentation as FFDM images to radiologists, they will be ‘reconstructed’ for DBT purposes and may then have further processing before presentation.

This protocol starts with a philosophy section in which the thoughts behind tests are explained. Subsequently the different test procedures are described, and terms and definitions can be found in the definitions section (Appendix III).

Philosophy

Digital Breast Tomosynthesis (DBT) is an active area of research and development. The first clinical systems have been introduced to the market and the first results of (European) breast cancer screening trials are available. Current DBT systems have very different characteristics, such as the angular range, step and shoot versus continuous motion of the tube, new target/filter combinations, new AEC working principles, with or without anti scatter grid, etc.

The clinical role for DBT systems has not yet been clearly defined. In addition it is not clear which design is optimal for different tasks. For example the advantages and disadvantages of using small or large angular ranges are not yet apparent. Will DBT systems be used primarily for diagnostic work-up, further assessment of suspicious findings or for breast cancer screening? Will DBT be used as a complementary method to FFDM or as a standalone screening technique? Answers to these questions will help to determine the limiting values for the tests proposed in the current document.

In practice, the implementation of DBT QC tests may differ from system to system. If DBT systems can perform both DBT and FFDM imaging, some measurements can be performed in FFDM mode. It must be verified that all relevant (exposure) conditions are similar (e.g. target material and filter thickness) and that in the case of detector tests the working of the detector is identical (e.g. binning of detector elements, response curve and detector corrections). The measurement of X-ray beam parameters is a practical challenge when a system is operating in DBT and may require special equipment. Examples of the problems faced are the pulsed exposure and the changing angle of incidence of the X-ray beam upon the breast support table as the tube moves. These challenges make measurements in DBT mode of tube voltage, tube output and HVL impossible with most current kVp and dose measuring equipment.

In developing QC procedures, it is important to consider the type of images available for analysis. For example, on some systems projection images are available, while on other systems they are not available or do not exist.

This protocol is intended for use on all DBT systems. We ultimately aim to provide limiting values guaranteeing proper performance for the different applications of DBT. Because of the differences in DBT systems mentioned above, and the principle that the same performance parameters should be measured on all systems, system performance tests are performed using the reconstructed tomosynthesis image. The benefit of this approach is that the image reconstruction is included in the QC test. However, there are some detector and system tests that have to be performed using projection images, as there is no validated method of measurement using reconstructed tomosynthesis images. For scanning geometry systems projection images are not available and alternative tests or testing in alternative imaging modes need to be investigated. Some QC tests, like the evaluation of artefacts caused by the image receptor, may be performed more easily in FFDM mode (if available) or in projection images.

In FFDM, images with the DICOM tag ‘For processing’ are used for QC analysis. In these images pixel values are assumed to have a linear relationship to receptor dose (or can be linearized), and to be shift invariant. The pixel values in reconstructed DBT focal planes are somehow related to tissue density but a well defined relationship with attenuation does not exist (like the Hounsfield units in CT imaging). It is not yet known to what extent a DBT system can be assumed to be shift invariant. Furthermore, image reconstruction algorithms can produce region-specific SDNR and spatial resolution.

Therefore, image quality assessment using contrast detail approaches or linear system theory metrics are a challenge. This is a topic under investigation.

The system should fulfil the requirements regarding breast tomosynthesis systems in the DICOM standard for DBT systems.

It is noted that for testing purposes a special QC mode incorporating the image reconstruction but excluding image processing techniques like artefact reduction and additional breast specific image processing techniques for visualization is necessary. Alternatively it must be possible to turn these image processing techniques off.

Zero degree angle stationary mode: For dose, HVL and tube voltage measurements a stationary mode at the zero degree angle is required for full-field geometry giving the same exposure as in DBT mode but without the tomosynthesis movement. All full-field geometry DBT systems should have this mode available. In this mode it must be possible to select the same X-ray spectra as used in DBT mode.

For scanning slot geometry systems the tomosynthesis mode MUST be used in dosimetry measurements to obtain accurate results.

The series of unprocessed projection images in zero degree stationary mode must be supplied with all appropriate detector corrections and flat-fielding in an easily accessible DICOM format.

Availability of projection images: Some QC tests can only be performed using projection images. On all DBT systems using a full-field geometry the **unprocessed** projection images must be made accessible for QC purposes, these have to be provided in easily accessible format e.g. a 'DICOM for processing' file for each projection image. It must be possible to restore the order of the images in the series of projections. All tags regarding the exposure and tags used for the identification of the image should be filled in.

On scanning geometry DBT systems projection images may not exist and therefore cannot be supplied. For these systems which inherently do not have projection images, the evaluation of system stability might be performed using simple backprojection images. These images should fulfil the DICOM standard for DBT systems.

The requirements of DBT systems regarding aspects of image quality are not yet known. Therefore limiting values are not given in this preliminary QC protocol, but in some cases reference values are given. An example of such reference values are those given for average glandular dose. The reference values are identical to the limiting values from the European Guidelines for FFDM. These limiting values have been chosen as reference values because the benefit of DBT in terms of cancer detection, versus the cost in terms of radiation dose is not yet clear. Applying too many restrictions at an early stage in the development of DBT may lead to a suboptimal dose-image quality balance. However, exceeding the limiting values of 2D mammography should only be accepted if clear benefit for the women is expected.

All relevant exposure information for individual projections should be available from the DICOM image header, including angular range of movement during projections, angular spacing between projections, and the distribution of the X-ray exposure between projections. Manufacturers should also provide the following information: focal spot - detector distance, focal spot-centre of rotation distance, exposure parameters and exposure time per projection for different beam loads, total scan time (with and without initial pre-exposure).

The bad pixel map applied to the detector when used in tomosynthesis mode should be made available to the user.

It is noted that for some systems the first image in the series of projections is the pre-exposure in zero degree position or in the largest angle position, for other systems the first image is the projection image in largest angle position. It should be ensured that the correct image is used in stability measurements, i.e. the first projection image for which the exposure is determined by the Automatic Exposure Control.

Some vendors consider to offer DBT systems with a variable exposure per projection image. If such systems are introduced it is important to check the exposure for each projection as this might influence both dose calculations and image quality.

Lag and ghosting between projection images might influence the image quality of the reconstructed DBT image. In future versions of this protocol, QC tests might be introduced to quantify the amount of lag and ghosting.

1 X-ray generation

1.1 Focal spot size (optional)

Method: The method for measuring the focal spot size is described in the 4th edition of the European Guidelines. Use the zero degree angle stationary mode image or an FFDM image for evaluation of focal spot size.

Remark: the focal spot size measurement can only be performed in FFDM mode if the same focal spot is used as in DBT mode.

Limiting values: For reference purposes
Frequency: Optional at acceptance, if image quality problems occur
Equipment: Suitable focal spot size phantom

1.2 Focal spot motion

For DBT systems in which the focal spot is in motion while the target is emitting x-rays, the distance that the focal spot travels during the exposure is an important parameter needed when determining the geometric unsharpness due to focal spot motion for a given object. This test applies to systems with x-ray tube motion during exposure. In Table 1 the focal spot to centre of rotation (h) and angular range of the system ($2\theta_m$) are given for currently available DBT systems and some prototype systems.

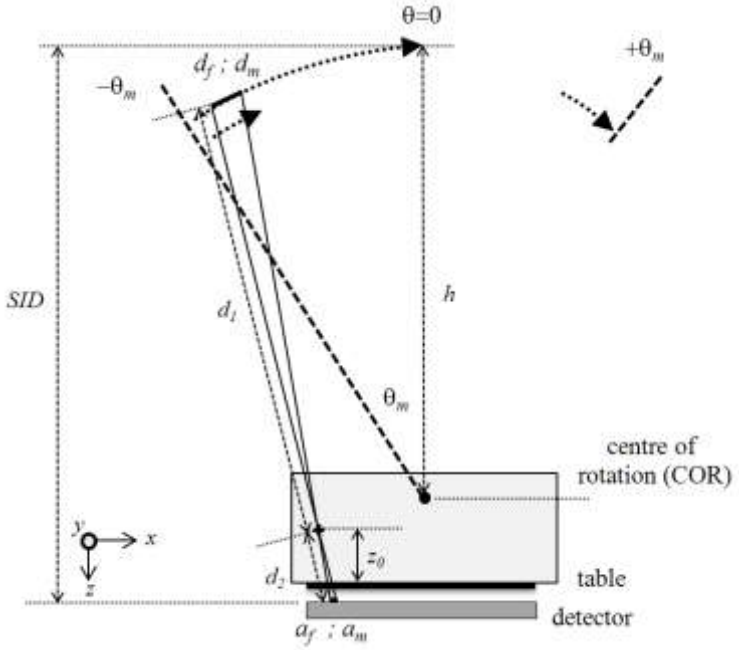

Figure 3 Definition of distances for calculation of focal spot motion. The term d_f is the dimension of the focal spot, the term d_m is the extended focal spot size due to motion of the anode during exposure (for systems with tube motion during exposure). The term d_1 is the distance from the focus to the object of interest, the term d_2 is the distance from this object to the detector entrance plane. As an example, geometric unsharpness is shown for an object at some height z_o above the breast support table.

Method: Measure the projection exposure time (t_{proj}) for typical current-time product settings found during the AEC object thickness compensation tests, using the zero degree stationary mode if necessary, and the time for a complete scan (t_{scan}). These figures can also be taken from DICOM header data if accurate and if available.

The focal spot motion length can be calculated using the equation:

$$d_m = 2h\theta_m \frac{t_{proj}}{t_{scan}} \quad (1)$$

Focal spot motion length (d_m) should be compared against focal spot size (typically 0.45 mm at the reference position) to give an idea of the influence of geometric unsharpness due to focal spot motion.

Remark: The blurring, expressed as the projected focal spot travel length (a_m) of an object at some point z_0 above the breast support table from the extended focal spot size due to focal spot motion (d_m) can be calculated using lengths d_1 and d_2 as:

$$a_m = d_m \frac{d_2}{d_1} \quad (2)$$

Limiting values: For reference purposes; The exposure time value from the DICOM header should be within 10% of the measured value (provisional).
Frequency: At acceptance or after a software update that changes exposure times
Equipment: A suitable exposure time meter

1.3 Alignment and collimation checks

Method: Position X-ray rulers on the bucky to mark the chest wall and lateral edges of the detector as indicated by the light field or lines on the breast support table as shown in figure 4. As the exact position of the edge of the detector is not known, this information is obtained from the image of the rulers. Mark the middle of four pieces of self developing film and position them on the bucky with the mark aligned with the X-ray ruler. Make an exposure to give sufficient blackening of the film, without saturating the detector. This may be achieved by making multiple exposures, or by placing an attenuating material (for example a 3mm thick aluminium plate) between the self-developing film and the detector and using a large exposure. Evaluate the coincidence of the X-ray field and the tomosynthesis image by finding the position of the X-ray field relative to the light beam from the self developing film, and the position of the light beam relative to the image from the image of the X-ray rulers in the reconstructed focal plane in which the rulers are in focus. It may be helpful to examine the projection images.

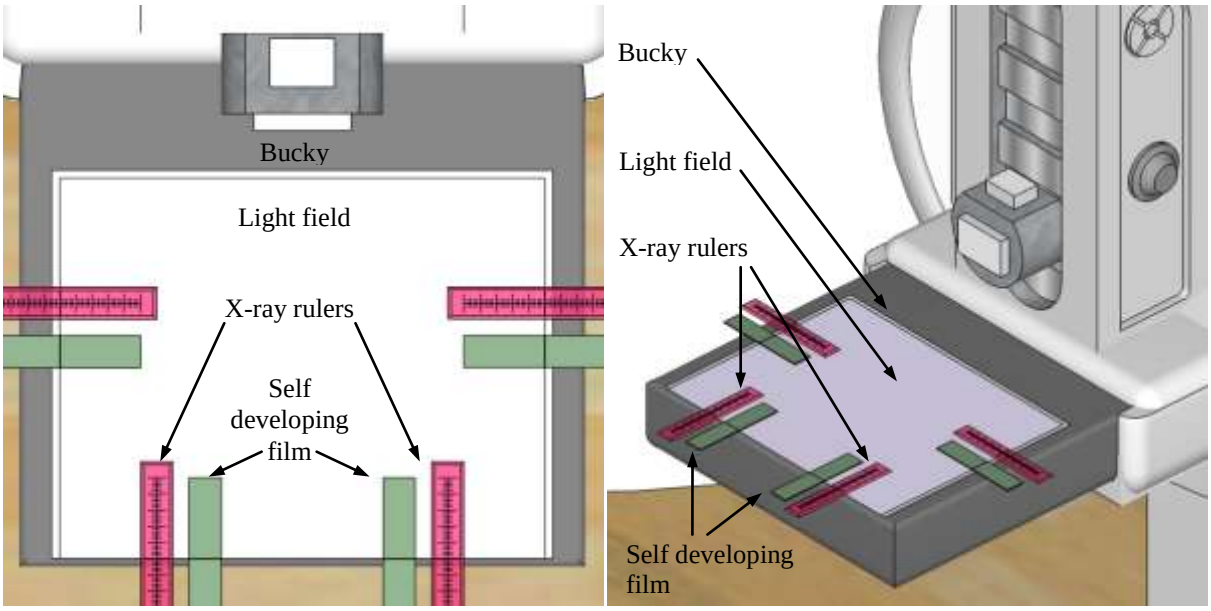

Figure 4 Set-up for measuring coincidence of reconstructed and irradiated volume on the bucky, top view and 3D view.

Limiting values: Chest wall side: X-ray field must extend no more than 5 mm beyond the edge of the image receptor (using projection images)/reconstructed tomosynthesis image. At lateral sides the X-ray field should not extend beyond the primary beam stopper in the bucky

Frequency: At acceptance and every six months
Equipment: X-ray rulers, self developing film

1.4 Tube output

For measuring tube output, a distinction is made between systems that have full-field geometry and scanning geometry. A description of the different geometries is given in the introduction of this protocol and in Dance et al 2011.

Method: Measure the tube output for all clinically used target filter combinations and relevant tube voltages. It is adequate to interpolate between tube voltage measurements. Repeat the measurement of the tube output of the spectrum used for the standard test block in the clinically used AEC mode 5 times to check short term reproducibility.

- For a system with a **full field geometry**: Position the dose meter within the X-ray field 60 mm from chest-wall side underneath and in contact with the compression paddle and measure the incident air kerma in **the zero degree angle stationary mode**. The dose meter should be positioned on a line extending from the tube focal spot to a point on the mid-line of the breast support table 60 mm from the chest wall edge. If the dose meter has back scatter correction the recommended position is directly on the breast support with the paddle in contact. If the dosemeter is not corrected for backscatter, precaution has to be taken as suggested in the dosimeter manual.

- For the **scanning geometry**: Position the dose meter on the midline of the bucky surface and 60 mm from chest-wall side. Measure the incident air-kerma for the **scanning** beam.

Note: In zero degree angle stationary mode the measured tube output might differ slightly from the FFDM mode due to the pulsed exposure. At acceptance a comparison could be made between the tube output during a tomosynthesis series and using FFDM mode.

Limiting values:	No limiting values. Tube output is measured for dosimetry purposes only. Tube output of 5 consecutive measurements (reproducibility) should be within 5% of the average tube output.
Frequency:	Every 6 months
Equipment:	Dose meter with suitable calibration

1.5 Tube voltage and beam quality

The beam quality of the emitted X-ray beam is determined by tube voltage, target material and filtration. Tube voltage and beam quality are used to calculate average glandular dose.

1.5.1 Tube voltage (optional)

Method: The method for measuring the tube voltage is described in the European Guidelines, 4th edition. Perform the measurements in the zero degree angle stationary mode. Perform at least 5 measurements covering the range of tube voltages used clinically. The reproducibility is measured by making 5 repeat exposures at one fixed tube voltage that is used for the standard test block

Note: In DBT mode, the measured tube voltage might differ slightly from the FFDM mode due to the pulsed exposure in DBT mode.

Limiting values:	Accuracy for the range of clinically used tube voltages: $< \pm 1$ kV Reproducibility: $< \pm 0.5$ kV
Frequency:	Every 6 months
Equipment:	Suitable tube voltage meter

1.5.2 Half Value Layer (HVL)

The Half Value Layer (HVL) can be calculated by inserting thin aluminium filters into the X-ray beam and measuring the attenuation. Perform the measurements in the zero degree angle stationary mode.

Method: Position the dosimeter at the reference position. Place the compression paddle as high up as possible between focal spot and the bucky. Limit the X-ray field to the area of the dosimeter. Perform measurements for each clinically used target filter combination. Sample the tube voltage range such that at least 3 measurements are performed for each clinically used target filter combination, unless fewer than 3 tube voltages need to be measured. Make an exposure with the compression paddle in place and without an aluminium filter and repeat the exposure twice with different thicknesses of aluminium filter placed on the compression paddle. The thicknesses of the aluminium filters should be chosen such that the measured incident air kerma levels are just above and below half the incident air kerma measured without filter.

Determine the HVL using equation (3):

$$HVL = \frac{X_1 \cdot \ln\left(\frac{2 \cdot Y_2}{Y_0}\right) - X_2 \cdot \ln\left(\frac{2 \cdot Y_1}{Y_0}\right)}{\ln\left(\frac{Y_2}{Y_1}\right)} \quad (3)$$

In this equation Y_0 is the air kerma reading without additional attenuation and Y_1 and Y_2 are the air kerma readings with added aluminium filter thicknesses of X_1 and X_2 respectively.

Note: In DBT mode the measured HVL might differ slightly from the FFDM mode due to the pulsed exposure in DBT mode.

Note: Filters used in DBT should be tested at least once in DBT mode and the results compared to those with the same filters in 2D FFDM

Limiting values:	No limiting values, only measured for the calculation of average glandular dose
Frequency:	At acceptance and after replacement of the X-ray tube
Equipment:	Suitable dose meter

1.6 Exposure distribution per projection image (optional)

The aim of this test is to measure the exposure distribution over the projections. This may be constant for some designs, whereas other DBT systems may vary the air kerma per projection according to some defined regime.

Method: If the dosimeter has a suitable waveform option and if there is a zero degree stationary mode, incident air kerma for each individual projection image can be determined. Position the dosimeter on a line extending from the tube focal spot to a point on the mid-line of the breast support table 60 mm from the chest wall edge. Initiate an exposure in zero degree angle mode and measure the incident air kerma for each projection image. Use clinically relevant exposure parameters for the standard test block.

Verify whether the distribution of the doses conforms to the description in the DICOM header of the images or to the description at the console.

Note: Depending on the design of the AEC and the angle of the pre-exposure, the measurement in the zero degree angle stationary mode might give slightly different results to those obtained with a moving tube.

Note: The exposure distribution per projection image might vary with thickness.

Limiting values:	Manufacturers specification
Frequency:	At acceptance
Equipment:	Dosimeter with suitable waveform option

2 AEC-system

If multiple AEC modes are used clinically, all modes must be measured at acceptance and after upgrade of the AEC software.

2.1 Guard timer/security cut-off

The security cut-off protects the patient, the exposure is terminated after the pre-exposure (or in the first milliseconds of the exposure) because the image quality which the AEC aims for, cannot be achieved. The guard timer protects the x-ray tube from reaching or exceeding its heat-loading capacity to prevent damage to the X-ray tube.

Method: Make an exposure in the clinically used AEC mode with a highly attenuating object covering the AEC part of the image receptor. Record the current-time product value at which the exposure is terminated.

Warning: An incorrect functioning of the back-up timer and security cut-off could damage the tube. To avoid excessive current–time product (mAs) consult the manual for maximum permitted exposure time.

Limiting values:	The guard timer and/or security cut-off should function according to specifications
Frequency:	Yearly
Equipment:	Suitable high attenuation object e.g. metal plate.

2.2 Short term reproducibility

Method: Position a standard test block on the bucky and initiate an exposure in the clinically used AEC mode. Record the exposure settings. Repeat this procedure 4 times. Measure the average pixel value and standard deviation in the reference ROI in the first projection image and calculate linearized SNR. Calculate the variation in current–time product (mAs) and in SNR.

Limiting values:	Variation in total current–time product (mAs) < 5%, variation in SNR < 10%.
Frequency:	Every six months
Equipment:	Standard test block

2.3 Long term reproducibility

Method: Position the standard test block on the bucky and initiate an exposure in the clinically used AEC mode. Record the exposure settings. Measure the average pixel value and standard deviation in the reference ROI in the first projection image and calculate SNR. The exposure is repeated a number of times during the QC test . Average pixel value, SNR and exposure settings are tracked over time.

Limiting values:	The variation in current–time product (mAs), average pixel value and SNR in the reference ROI should be <10% and exposure factors should remain unchanged.
Frequency:	During Daily/weekly, after system calibration and after maintenance
Equipment:	Standard test block

2.4 AEC performance

This test uses readily available QC equipment. More advanced tests are under development.

Method: Automatic exposure control performance for different object thicknesses should be measured for PMMA plates in the thickness range from 20 to 70 mm (steps of 10 mm) and the standard test block in all clinically used AEC modes. Position the compression paddle at the height given in table 2 to obtain the thickness of the equivalent breast with similar attenuation to the PMMA slabs, see figure 5a and 5b and table 2.
Alternatively, a combination of PMMA and PE slabs can be used to mimic the thickness of a standard breast with the same attenuation, see table 3.

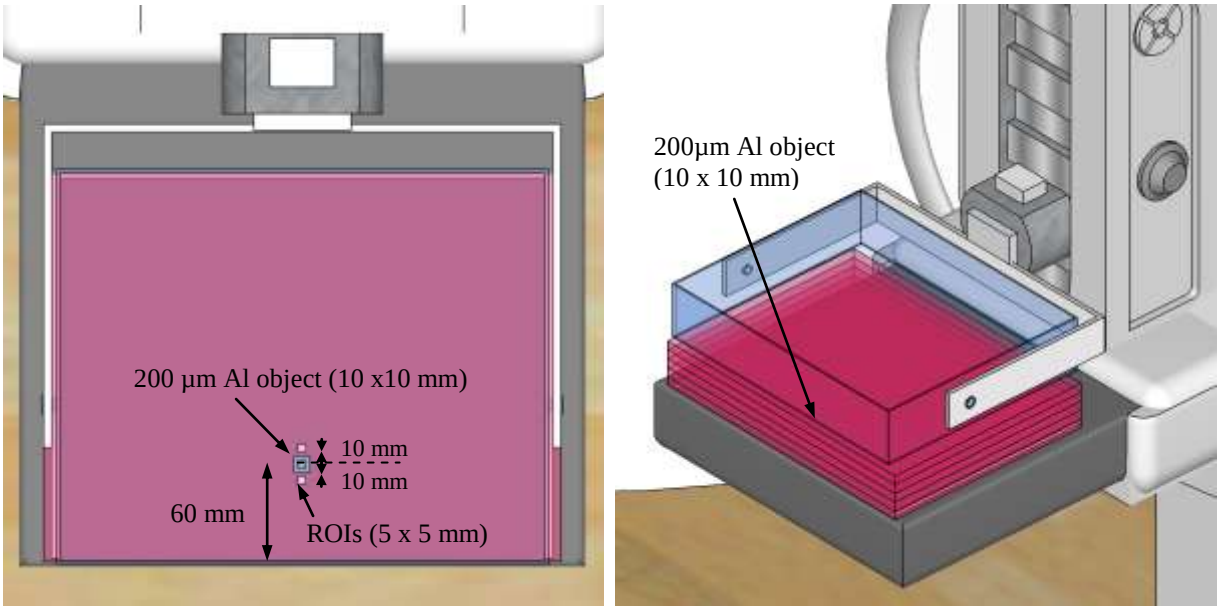

Figure 5a Setup for the breast thickness and composition measurements (50 mm PMMA + 10 mm air gap), top view and 3D-view.

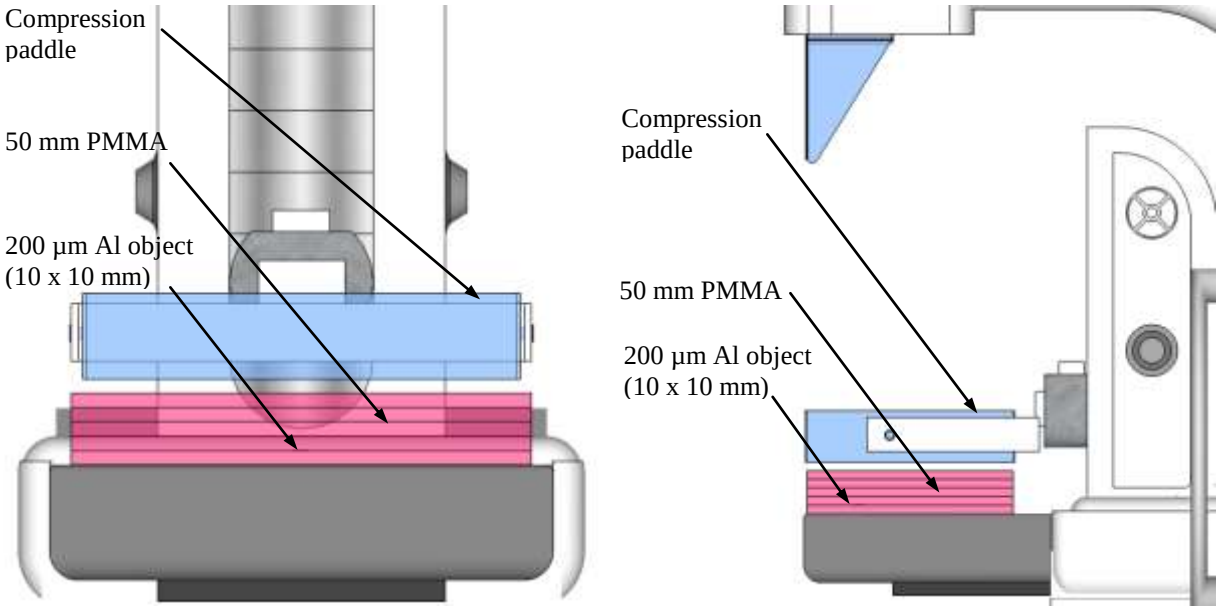

Figure 5b Setup for the breast thickness and composition measurements (50 mm PMMA + 10 mm air gap), front and side view.

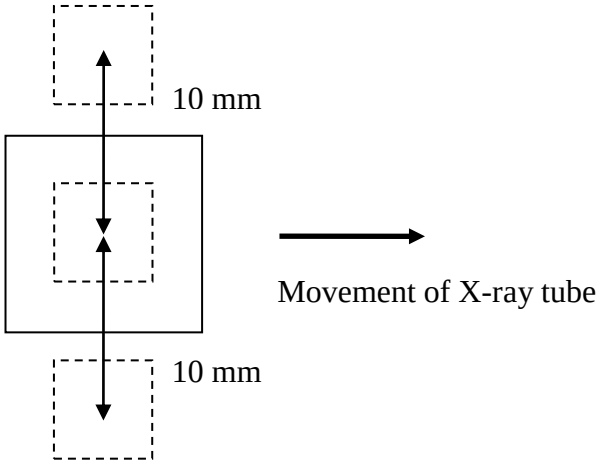

Figure 5c The ROI positions to calculate SDNR.

Image two 10 mm thick stacked PMMA plates covering the whole image receptor, with an aluminium sheet of dimensions 10x10 mm and 0.2 mm thick wedged between the plates. Position the aluminium at a distance of 60 mm from chest wall side and centred laterally, as shown in Figure 5a. Image the stack of PMMA in the clinically relevant AEC mode, if necessary the image can be made in manual mode with settings as close as possible to the clinical AEC settings for the equivalent breast thickness.

Table 2 Height of the compression paddle when using different PMMA thicknesses.

PMMA thickness (mm)	Height of the compression paddle (mm)
20	21
30	32
40	45
45	53
50	60
60	75
70	90

Table 3 Thickness of PMMA and PE to match the attenuation of the standard breast with similar thickness.

Standard breast thickness (mm)	PMMA thickness (mm)	PE thickness (mm)
20.0	20.0	0.0
30.0	27.5	2.5
40.0	30.0	10.0
50.0	32.5	17.5
60.0	32.5	27.5
70.0	32.5	37.5
80.0	32.5	47.5
90.0	35.0	55.0

Repeat this measurement for the PMMA thicknesses according to Table 2 column 1 by adding additional slabs of PMMA on top of the stack. The compression paddle should be positioned as given in Table 2 column 2. This is achieved by leaving an air gap between the PMMA plates and the compression paddle. If compression is necessary to make an exposure, then spacers may be used, but they must be positioned such that they do not reduce transmission of X-rays to the central and chest wall regions of the image at any tube angle. This may be achieved by placing spacers along the back edge of the PMMA.

Alternatively a combination of PMMA and PE slabs can be used to simulate the standard breasts. The required thickness of PMMA and PE is given in table 3, all PMMA slabs should be at the bottom of the stack, all PE slabs on top of the PMMA stack.

Position a 5 mm x 5 mm ROI in the centre of the image of the aluminium sheet in the first projection image, and position two 5mm x 5mm ROIs in the background areas on the chest wall and nipple sides of the aluminium sheet, see Figure 5c. The centres of both background areas should be at a distance of 10 mm from the centre of the ROI in the aluminium sheet. If the focal plane has a significant degree of non-uniformity it may be necessary to compensate for this by using ROIs subdivided into 1mm x 1mm elements and using the averages of the mean pixel values and standard deviations from the elements. Measure the pixel values and standard deviations in the ROIs.

Calculate PV(background) and SD(background) according to:

$$\mathrm{SD(background)} = \frac{\sum_1^2 \mathrm{SD(ROI_n)}}{2} \tag{4}$$

$$\mathrm{PV(background)} = \frac{\sum_1^2 \mathrm{PV(ROI_n)}}{2} \tag{5}$$

Calculate the SDNR of the aluminium object:

$$\mathrm{SDNR} = \frac{PV(signal) - PV(background)}{\mathrm{SD(background)}} \tag{6}$$

Limiting values: Not yet established, SDNR values are calculated for reference purposes, to allow stability testing
Frequency: Every six months
Equipment: Aluminium sheet (10mm x 10mm, 0.2 mm thick), seven PMMA slabs of 10 mm thickness, one PMMA slab of 5 mm thickness

2.5 Exposure duration per projection and total scan duration

Exposure time per projection and total scan time are important parameters of system performance (see focal spot motion tests). The exposure time per projection may lead to focal spot motion unsharpness. Long scan times may also lead to an increased risk of patient motion.

Method: Position the standard test block on the bucky and make an exposure in the clinically used AEC mode. Measure the duration of each projection image and the time between the start of the first and the end of the last exposure. If the exposure time meter interferes with the exposure chosen by the AEC, the standard test block should be imaged without the exposure time meter. The exposure factors should be recorded and simulated afterwards in manual mode with the exposure time meter in the X-ray beam.

Optionally, by using the DICOM header of the images made in paragraph 2.4 ´AEC performance´, the exposure times of images at different simulated breast thickness can be calculated and recorded.

Limiting values:	No limiting values set, clinical evaluations are required to evaluate potential motion artefacts and the impact of occasionally long pulse widths. Measured values can be used to ensure stability and similar settings on the same type of system.
Frequency:	Exposure duration per projection: acceptance test, every six months, Total scan time: at acceptance and if changes have been made in the acquisition of images.
Equipment:	Exposure time meter with a waveform option

2.6 Response to local and global variations in breast density

Most systems measure the attenuation of the imaged object during a pre-exposure. The areas with highest attenuation in the clinically relevant part of the image should determine the exposure factors for imaging. We require that the SNR in the projection images is adjusted to the (relatively large) regions with highest density.

Position a stack of 40 mm PMMA on the bucky. Put spacers on top of the stack, such that the compression paddle is positioned at a height of 50 mm above the breast holder (compression force can be applied), see figure 6a and 6b. The spacers should not cover the part of the detector in which exposure factors are determined (AEC sensor area) for all projection images. This simulates the attenuation of a 50 mm thick fatty breast. On the compression paddle, a first small PMMA plate representing an areas with higher glandularity (dimensions: 20 mm x 40 mm, 2 mm thick) is positioned in the central part of the detector with its lower edge 50 mm from chest wall side, see figure 5 and 6 (It must be ensured that this is within the AEC sensor area. If this is not the case, another position should be chosen). Make an exposure in the clinically relevant AEC mode and record the exposure factors. Add another small PMMA plate on top of the previous one and repeat the procedure until a total thickness of 14 mm small PMMA plates has been added. This is approximately equivalent to a 50 mm thick standard model breast with 100% glandularity in the central region, see section 6.1.

Alternatively a combination of 20 mm thick PMMA and 30 mm thick PE slabs can be used to mimick the attenuation of a 50 mm fatty breast. The 30 mm PE must be positioned on top of the 20 mm PMMA In this case spacers do not have to be used. On the compression paddle, a first small PMMA plate representing an areas with higher glandularity (dimensions 20 mm x 40 mm, 2 mm thick) is positioned in the central part of the detector with its lower edge 50 mm from chest wall side, see figure 5 and 6 (It must be ensured that this is within the AEC sensor area. If this is not the case, another position should be chosen). Make an exposure and record the exposure factors. Add another small PMMA plate on top of the previous one and repeat the procedure until a total thickness of 14 mm small PMMA plates has been added (this approximately equals 100% glandularity).

On the first projection image, measure pixel value and standard deviation in the area of extra attenuation (20 mm x 40 mm PMMA plates) with a ROI of 5 mm x 5 mm. Calculate SNR in the first projection image of each tomosynthesis acquisition and calculate the average SNR for all

these first projection images. It should be checked whether the exposure of the tomosynthesis acquisitions is increased with additional PMMA object thicknesses. For this the following value can be used as guidance: the SNR of each projection image should be within 20% of the average SNR (provisional).

Guidance	The SNR of each first projection image should be within 20% of the average SNR. (provisional) Further research is needed before limiting values can be established.
Frequency	Every six months or after AEC software upgrades
Equipment	Four PMMA plates (dimensions at least 150 mm x 180 mm, each 10 mm thick), two spacers (10 mm thick), seven 20 mm x 40 mm PMMA plates (2 mm thick)

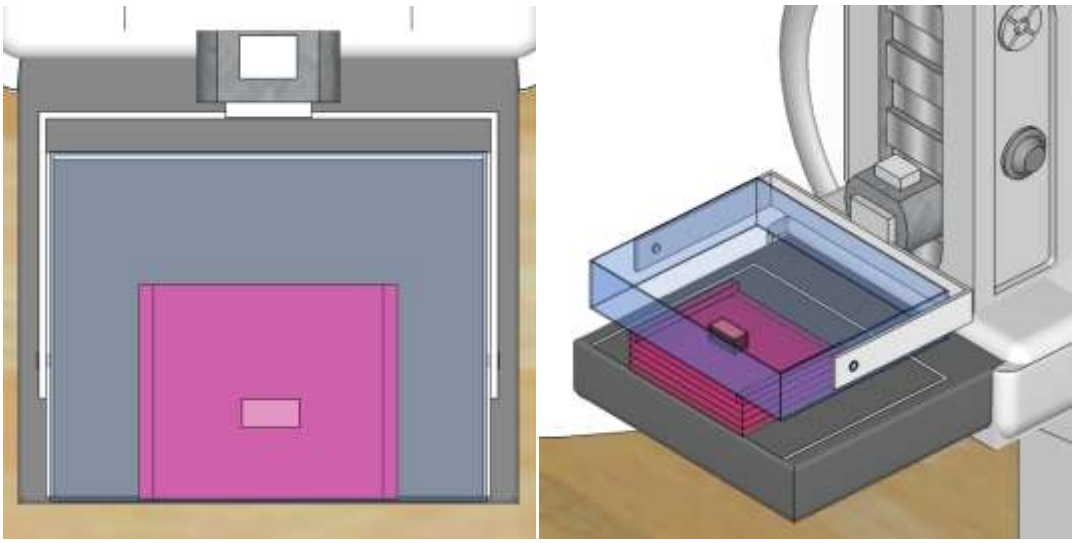

Figure 6a. Setup for the local dense area measurement, top view and 3D view.

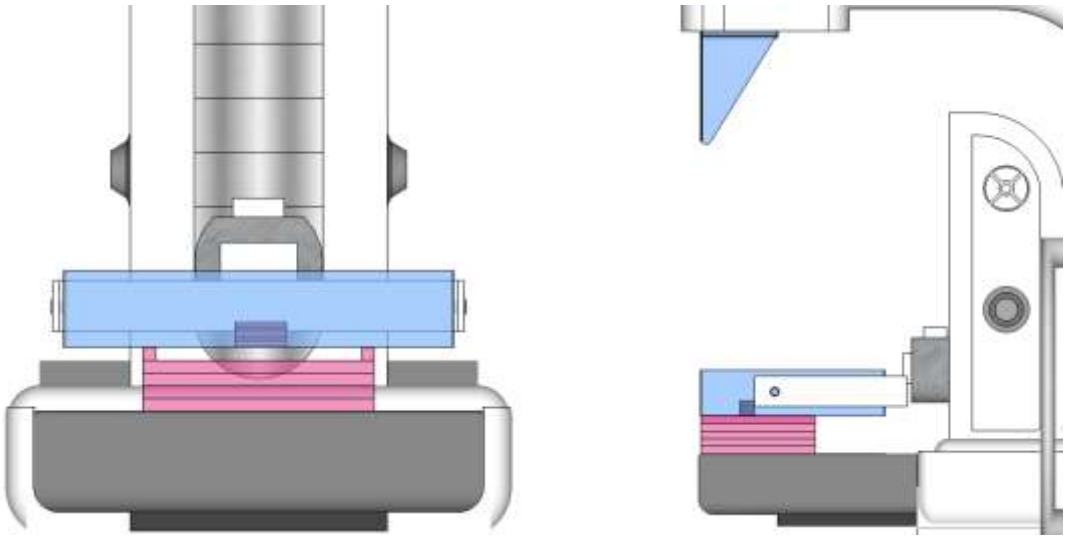

Figure 6b. Setup for the local dense area measurement, front view and side view.

3 Compression

3.1 Compression force

Method: Measure the motorised compression force with a compression force test device (use compressible material e.g. a tennis ball to protect the bucky and compression device). Both the applied compression force and the accuracy of the indicated compression force are verified. Examine the compression paddle visually for cracks and sharp edges.

Record the maximum compression force and the compression force after 1 minute of compression. Report any visual damage of the compression device.

Limiting values:	Maximum motorized compression force may not exceed 200 N and must be at least 130 N. The decline in compression force within 1 minute may not exceed 10 N. No sharp edges and cracks in the compression paddle should be present.
Frequency:	Yearly
Equipment:	Compression force test device

4 Image receptor

4.1 Image receptor response

4.1.1 Response function

Response function is measured in DBT projection images or in projection images acquired in zero degree angle stationary mode.

Method: Remove the compression paddle and any other removable parts from the X-ray beam. Position a 2 mm thick aluminium plate as close as possible to the X-ray tube.

Set the target/filter combination and tube voltage which is chosen in fully automatic mode for the standard test block. In manual mode, set the minimum current-time product (mAs) value. Image the aluminium plate. Increase the current-time product and repeat the acquisition. Acquire several scans (typically 8 current-time product values) over the available range, increasing the current-time product by a factor of approximately 1.4 (if possible) between exposures.

It is optional to repeat the measurement for all target-filter combinations, with a clinically relevant tube voltage for each combination.

It is optional to measure or calculate, from tube output measurements, the incident air kerma on the detector surface and use it instead of current–time product (mAs) in this evaluation.

Measure the mean pixel value and standard deviation in the standard ROI on the first projection image of the zero degree angle stationary mode or the first projection image in DBT mode to limit the influence of lag and ghosting in the measurements. Plot mean pixel value against current-time product (or incident air kerma at the detector) and check whether the response function is according to manufacturer's specification.

Remark: Detector gain (the gradient term of the response function) is usually increased for DBT mode compared to standard 2D mammography mode, because of the lower exposure per projection used in DBT systems.

Limiting values: Results at acceptance are used as reference.
Frequency: Every six months
Equipment: 2 mm thick aluminium plate (99% purity), optional: suitable dose meter.

4.1.2 Noise analysis

Noise analysis is performed in DBT projection images or projection images acquired in zero degree angle stationary mode.

The aim of this test is to quantify the contribution of different noise components to the total image noise in order to provide additional information on the performance of the imaging system. This may assist in trouble-shooting if image quality problems occur.

General requirement: For systems with a non-linear response, the pixel data must be linearized before analysis.

Noise in images can be subdivided in electronic noise, quantum noise and structural noise (Bouwman 2009, Monnin 2014):

$$SD^2 = k_e^2 + k_q^2 * p + k_s^2 * p^2 \quad (7)$$

SD = standard deviation in reference ROI
k_e = electronic noise coefficient
k_q = quantum noise coefficient
k_s = structural noise coefficient
p = average pixel value in reference ROI

Electronic noise is assumed to be independent of the exposure level and arises from a number of sources: dark noise, readout noise, amplifier noise.

Structural noise is present due to spatially fixed variations of the gain of an imaging system. The flatfielding performed in DR systems will largely remove the effects of structural noise. Due to the limited number of images used for the flatfield mask and the associated noise in the mask, some structural noise remains. Furthermore flatfielding might not be performed for projection images individually, leading to some additional structural noise.

Quantum noise arises due to the variations in X-ray flux.

Method: The images acquired for measurement of detector response (section 4.1.1) are used for this test.

It is optional to repeat the measurement for all target-filter combinations, with a clinically relevant tube voltage for each combination.

Optional: Measure or calculate the incident air kerma on the detector surface from tube output measurements for all spectra to be able to plot against detector air kerma instead of pixel value.

Analysing steps:

1. Measure pixel value and SD in the reference ROI.
2. Linearize the mean pixel and SD values using the response function measured in paragraph 4.1.1.
3. Plot SD^2 against pixel value (or detector incident air kerma).
4. Fit a curve to the points using equation (7) and determine the noise coefficients

the calculated noise components can be used to plot pixel value (detector dose) against the percentage of the total relative noise for all noise components. In this graph the magnitude (in %) of all noise components is visualized for the range of pixel values (detector dose).

Note: Quantum noise may not be the largest noise component in individual projection images.

Limiting values:	Use the noise coefficients for reference purposes to verify stability and similar settings/quality on the same model of system.
Frequency:	Every six months
Equipment:	2 mm thick aluminium plate, optional: dose meter

4.2 Detector element failure

Method: Obtain the most recent "bad pixel map" for tomosynthesis mode from the system.

Remark: this map might differ from the bad pixel map in FFDM mode due to the differences in readout of the detector or pixel binning after readout.

Limiting value:	At present no limits have been established. It is suggested that the manufacturer's limits are used.
Frequency:	Every six months
Equipment:	None

4.3 Uncorrected defective detector elements

The uncorrected defective detector elements test is performed on projection images acquired in tomosynthesis mode or projection images acquired in zero degree angle stationary mode images.

Method: Make five images of the standard test block and determine whether any pixel deviates more than 20%(provisional value) in value compared to the average value in an ROI of 5 mm x 5 mm. Uncorrected defective detector elements show deviations in all projection images.

Limiting value:	No uncorrected defective detector elements should be visible and any pixel in an ROI of 5mm x 5mm should deviate less than 20% (provisional value) in value compared to the average value in this ROI.
Frequency:	Every six months
Equipment:	Standard 45 mm thick PMMA block

4.4 System projection MTF

The system projection MTF measurement is performed using DBT projection images.

The system MTF measured in the projection images includes the following sources of blurring: focal spot size, focal spot motion and detector MTF. The detector MTF includes the effect of blurring due to the x-ray converter, pixel size and detector binning. The system MTF measured in zero degree angle stationary mode includes the same blurring sources with the exception of focal spot motion.

The MTF in the tube travel direction may be strongly influenced by the effective size of the focal spot due to tube motion, which in turn depends on the exposure pulse length per projection image. Blurring (for some object) in the projection images due to focal spot size and focal spot motion depends on the position above the bucky. Hence, a system MTF in the projection images should be measured at a number of positions above the bucky, using the tube voltage, mAs so that the X-ray pulse length corresponds to the clinical situation which is simulated. This information can be found in the AEC test results, as a function of PMMA thickness. For example, placing the edge 70 mm above the table and using the x-ray factors for 70 mm PMMA gives an assessment of system projection MTF at a position towards the top of a 90 mm thick

breast. Blurring or resolution loss in the detector itself can be isolated by measuring MTF in FFDM mode or zero degree angle stationary mode with the edge on the detector housing.

Method: Remove the compression paddle. Position a 2 mm thick aluminium plate as close as possible to the X-ray tube to attenuate the whole X-ray beam. Place the MTF edge on the bucky at a small angle (~ 3^{O}) to the orientation of the pixel matrix, with the centre of the edge to be used on the midline at a distance of approximately 60 mm from the chest wall edge. Perform a DBT scan using the same beam quality as would be selected by the AEC for the standard test block. Ideally one would increase the current–time product (mAs) to three times the AEC value to reduce the influence of noise on the measurement, but it is likely that the exposure duration for each pulse would be increased which must be avoided, unless the system can increase the tube current and keep the exposure times constant.

A check should therefore be made to ensure that the pulse exposure time is typical of clinical values. Rotate the MTF edge through 90^{o} and repeat to obtain the MTF in the orthogonal direction. Alternatively the MTF can be measured in both directions in a single image using a suitable MTF test tool with two orthogonal edges. Repeat the pairs of orthogonal images with the edge positioned 40 mm and 70 mm above the table surface. To achieve this the MTF tool should be placed on low contrast supports (e.g. expanded polystyrene blocks positioned such that they do not influence the area used for MTF analysis or small plastic blocks) For routine measurements the MTF has only to be assessed at 40 mm height above the table surface. Calculate the MTF from the projection image closest to the 0° position (i.e. DICOM tag '0018,1530 Detector Primary Angle' ~0°), using appropriate software (e.g. OBJ_IQ_reduced as described in NHSBSP Equipment Report 0902). Re-bin the MTF data at $0.25mm^{-1}$ spatial frequency intervals. Find the spatial frequency for MTF values of 50% and 10%.

Options: collimate field to 100 x 100 mm if possible. Reposition the edge between DBT scans such that the horizontal edge and vertical edge are at the same position on the detector.

Remark: Some systems use some kind of pixel binning of the projection images. The binning used by the system should be noted as it is an important source of blurring. Note that some systems may save the projections binned or un-binned; it is possible that systems save un-binned projection images and bin these images before reconstruction. As such, this binning step can be considered as part of the reconstruction as it cannot be discriminated from a reconstruction filter.

Remark: If the temporal response of the x-ray detector (e.g. in terms of x-ray fluorescence or charge trapping and release in a photoconductor) is not sufficiently fast with respect to the projection image acquisition rate then signal carry over (lag) between projections will be seen. The cumulative effect of the lag is changing brightness near the region of the edge. This results in a ramp function superimposed on the high value part of the edge spread function and ultimately leads to a reduction in MTF at low spatial frequencies.

Remark: Edge images acquired for systems with a non-linear detector response curve must be linearized before MTF calculation while linearization is not essential for systems with a linear detector response curve. The generic (standard) response curve, as measured using 2 mm Al in section 4.1.1, can be used for all the edge images, regardless of beam quality setting.

Limiting values: Record the spatial frequencies at 50% and 10% points on the MTF curve. These values should be within 10% of the baseline values.

Frequency: At acceptance: Measure at the bucky surface and at 40 and 70 mm above the bucky table. Every six months: Measure at a height of 40 mm above the bucky table.

Equipment: A 1 mm thick steel sheet of minimum dimension 50 x 50 mm^2 with straight edges. Appropriate MTF calculation software, 2 mm thick aluminium plate.

4.5 Lag-ghosting

Under development.

5 Image quality of the reconstructed image

Image quality measurements are essential for the evaluation and optimization of breast tomosynthesis systems. Sufficiently high image quality is required at acceptance and should be maintained during the lifetime of the equipment. These image quality measurements in breast tomosynthesis should represent relevant clinical tasks. Examples are detection of microcalcifications and masses in mammographic backgrounds.

The current phantoms used in FFDM cannot be used to assess image reconstruction because they do not include mammographic backgrounds. New 3D structured phantoms are being developed with some of them including objects for detection tasks. This detection can be evaluated via human observers or using model observers which are being developed. As soon as validated methods to test system performance are available they will be included in this protocol including fail/pass criteria.

Limiting values: Under evaluation.
Frequency: Every 6 months.
Equipment: validated phantom typically including mammographic 3D backgrounds and simulated clinical objects

5.1 Stability of image quality in the x-y plane

It is important to investigate in-plane and inter-plane stability of image quality. For now, it is advised to use the methods and phantoms as used in FFDM, such as the CDMAM and TORMAM phantoms. It is realized that the tests proposed in this section have been designed for FFDM and have problems/disadvantages when used on tomosynthesis systems.

It is emphasized that comparisons of performance between different models cannot be made using the current 2D phantoms. However these phantoms do have an important role in stability assessment and quantifying some aspects of image quality.

5.1.1 CDMAM phantom

Method: Image the CDMAM phantom in the middle of a 40 mm stack of PMMA using exposure factors as would be selected automatically for a 60 mm equivalent breast. Repeat 6 times, moving the phantom slightly between exposures. Score the reconstructed tomosynthesis images of the CDMAM phantom using human observers and calculate the CD-curve according to the supplement to the fourth edition of the European Guidelines.

For some DBT systems it is possible to score the focal plane where the image of the CDMAM phantom is in focus using CDCOM, in which case 8 to 16 CDMAM images should be used. It is advisable to ensure that the entire CDMAM is brought into focus in a single focal plane by careful positioning of the phantom to compensate for any tilt of the reconstructed focal planes relative to the breast support table. As CDCOM is designed to read images in the FFDM format,

it is necessary to extract the focal plane where the CDMAM is in focus from the reconstructed tomosynthesis image. Where there is significant low frequency non-uniformity in the reconstructed focal planes, flatfielding should be applied before automated reading using CDCOM. A suitable flatfielding algorithm involves cropping to the useful area of the CDMAM and padding out to achieve an image size equal to the nearest power of two. An appropriate filter such as a Butterworth filter should be applied in the frequency domain to remove the higher frequencies including the grid and contrast details of the CDMAM, using a fourth order filter with a cut-off of 5mm. The original image is then divided by the original image and the pixel values rescaled.

Note that the use of CDCOM for reading tomosynthesis images has not been validated by comparison with human reading (as in Young 2006) and converting the results of this automated analysis to predicted human values using the method described in the Supplement to the European Guidelines may not be correct. However, automated reading and analysis of tomosynthesis CDMAM images using software designed for 2D images may be a useful interim tool for monitoring the stability of DBT image quality.

Note: There are cases that the in-focus surface of each CDMAM phantom position differs owing to a slight tilt or piece-to-piece variations of the phantom. Therefore, when using CDCOM software for evaluation, it is advisable to score various focal planes near the plane in which most objects seem in focus visually. The best result should then be selected.

Limiting values: The measured contrast threshold values can be used as a reference Note: The limiting values for FFDM image quality measurements cannot be applied to DBT.
Frequency: Every 6 months.
Equipment: CDMAM phantom, PMMA plates

5.1.2 TORMAM phantom

Method: Image the TORMAM phantom on top of a 30 mm stack of PMMA using automatically selected exposure factors. Carry out a visual assessment of the image of the TORMAM. For this assessment it is necessary to use a primary display monitor under appropriate conditions, with window level and width and zoom functions adjusted to maximise visibility of the details. A scoring system may be used, where points are accumulated for discs, filaments and specks according to how clearly they are visualised. However such systems are highly subjective and likely to vary significantly between observers and between observations by the same observer on different occasions. Alternatively assessment may be made by comparison to a baseline image, recording whether the visibility of details in the image is the same, or better or worse than in the baseline image. When comparing against a baseline image the two images should be displayed simultaneously.

Note that for some systems the bucky is not parallel to the image receptor, but tilted slightly. To get all the objects of phantoms in focus in one focal plane requires to tilt the phantom with the same angle.

Limiting values: The visibility of details in a baseline image can be used as a reference Note: Standards for the visibility of details in a 2D TORMAM image cannot be applied to DBT.

Frequency: Every 6 months.
Equipment: TORMAM phantom, PMMA plates

5.2 Z-resolution

Tomosynthesis imaging of a 3D phantom containing 1 mm diameter aluminium spheres enables an assessment of the inter-plane spread of the reconstruction artefacts associated with each sphere. These artefacts appear in focal planes adjacent to the plane representing the actual height of the sphere. A measurement of the spread between focal planes of the reconstruction artefacts associated with a sphere can be regarded as a measure of inter-plane resolution or z-resolution. This measurement is dependent upon the size of the sphere. Reconstruction artefacts typically stretche the sphere into a faint line in the direction of tube motion. There is often also a shift in the position of the artefact in the adjacent focal planes, relative to the position of the sphere in focus, due to magnification effects. Therefore, when assessing inter-plane spread, it is not sufficient to include only those pixels in a vertical line through the position of the sphere in the reconstructed volume. Instead the vertical component of inter-plane spread is assessed, by plotting a profile through the maximum pixel value in the vicinity of the sphere from each of the adjacent focal planes.

A test phantom is used which contains several 1mm aluminium spheres in order to make simultaneous measurements at multiple positions across the field of view within a single image. Images acquired using the geometric test phantom (section 5.7) may be used for this purpose, enabling the two tests to be combined.

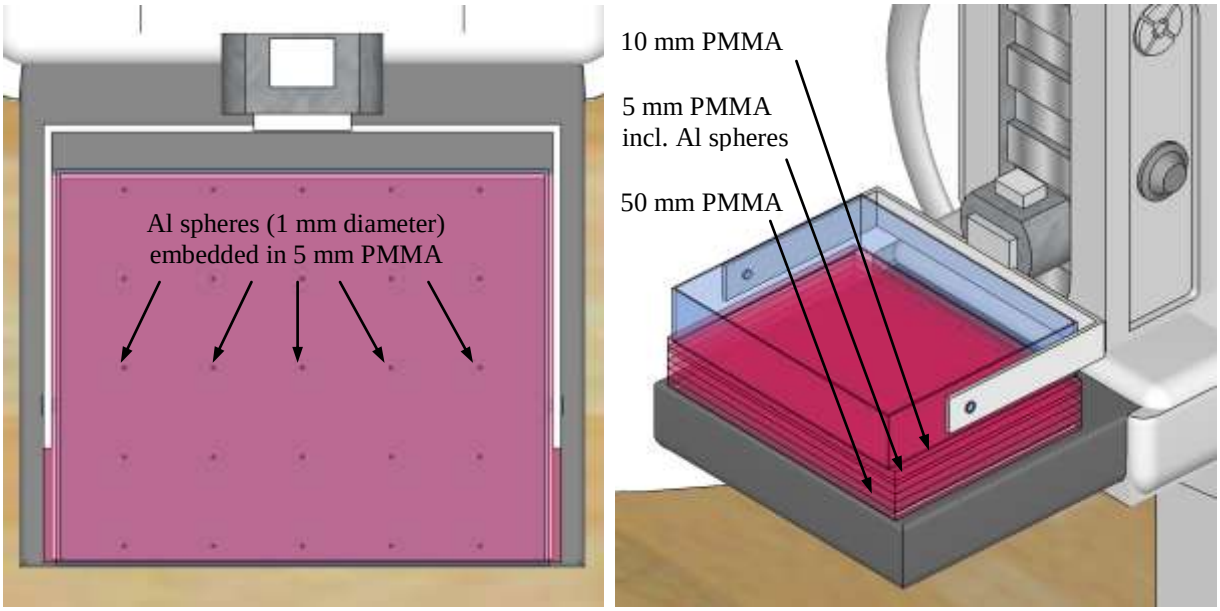

Figure 7a Setup for the evaluation of z-resolution (50mm PMMA + 5mm phantom), top view and 3D-view.

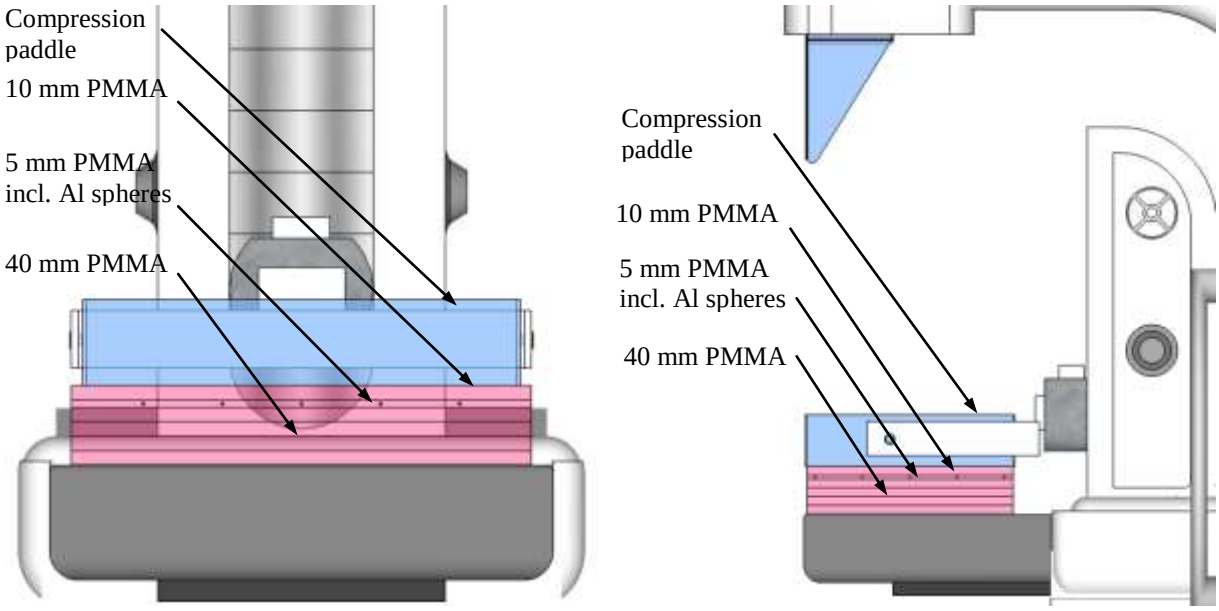

Figure 7b Setup for the evaluation of z-resolution (50mm PMMA + 5mm phantom), front and side view.

Method: Position six 10 mm thick slabs of PMMA on the bucky. Position the 5 mm thick phantom containing the aluminium spheres between the first and second slab and make an exposure in the clinically used AEC mode. Repeat with the aluminium spheres between the third and fourth slab and again between the fifth and sixth slab, see figures 7a and 7b.

A visual inspection is made of the appearance of artefacts and how they change and shift between focal planes.

Quantitative measurements are made of the vertical component of the artefact spread in terms of full width at half maximum (FWHM) and full width at quarter maximum (FWQM) measurements in the direction perpendicular to the detector surface. The half maximum value is taken to be the midpoint between the highest pixel value within the reconstructed image of the sphere and the average background pixel value taken from an artefact free region surrounding the sphere in the plane in which the ball is in focus.

The vertical spread of the artefact is not necessarily measured in a straight line through the reconstructed image: the maximum pixel value within the artefact for each plane perpendicular to the direction of the FWHM (or FWQM) is used, thus enabling allowance to be made for angulation and inhomogeneous spread of the artefact. Automated software or DICOM viewer tools are used to produce composite images of pixel maxima and reduce them to single lines of maxima, from which the vertical FWHM (or FWQM) is calculated either by linear interpolation or fitting a polynomial spline to the data. Where the shape of the vertical profile is complex it may not be sufficient to measure the FWHM, therefore it is advised to calculate FWQM also.

This analysis is most easily carried out by using dedicated software, which will be made available on the EUREF website.

Limiting values: To be determined, the FWHM and FWQM values can be used for reference purposes and to ensure stability and similar settings/quality of the same model of system.

Frequency: Every six months

Equipment: 5 mm thick phantom containing aluminium spheres (1 mm diameter), six 10 mm thick PMMA slabs

5.3 MTF in the x-y plane (optional)

The use of linear system theory metrics on reconstructed images is under debate. Especially for iterative reconstruction techniques, it is not known whether linear system theory metrics are valid. The relationship between these metrics and image quality of clinical reconstructed tomosynthesis (with structured backgrounds) is not known yet and might be complex. Currently the measurement of MTF in the x-y plane is proposed to monitor stability of the tomosynthesis system and to allow comparison of results obtained from systems of the same model.

The system MTF measured in the reconstructed planes (effectively the total system MTF for the focal plane in which the wire is located) includes all the sources of blurring in the system: detector MTF, and all additional sources of unsharpness and the reconstruction algorithm. DBT is a pseudo-3D technique and should ideally be measured using a method that gives the 3D MTF. The method given below does not give the 3D MTF but instead the in-plane MTF (x-y) in tube travel and chest wall-nipple directions.

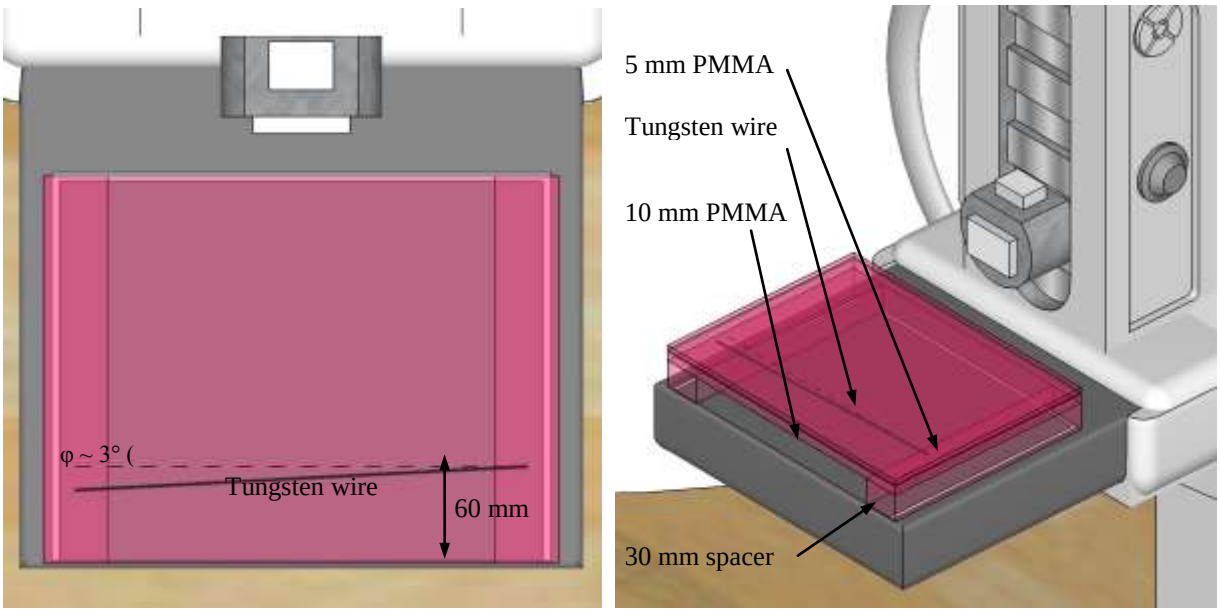

Figure 8a Setup for the evaluation of MTF in focal plane, top view and 3D-view.

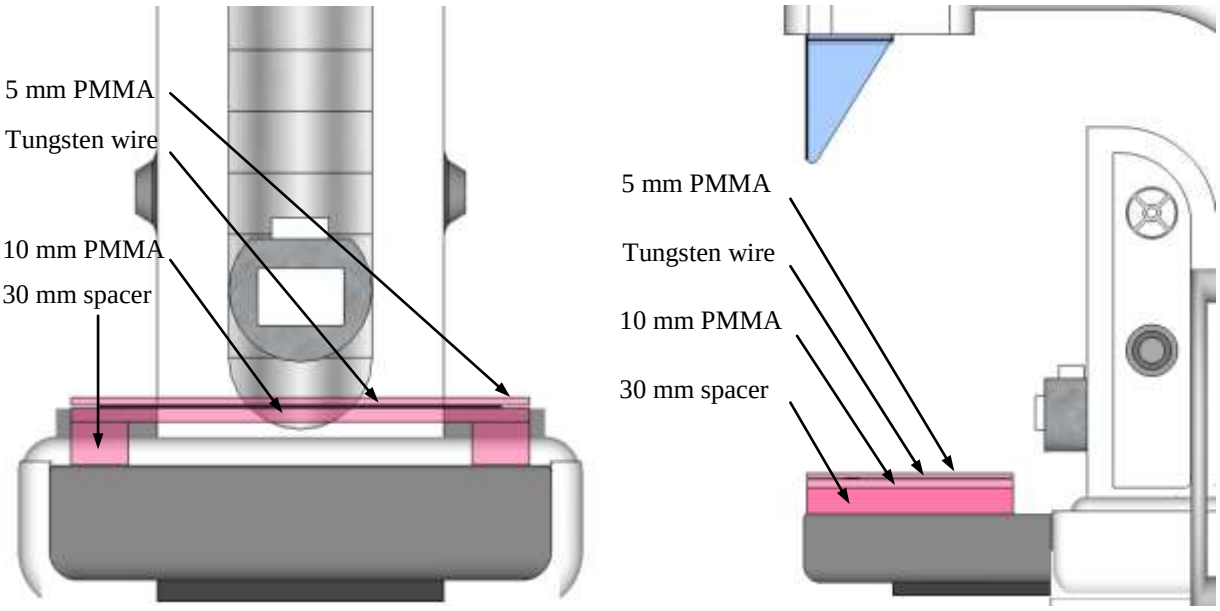

Figure 8b: Setup for the evaluation of MTF in focal plane, front and side view.

Method: In-plane MTF is measured using a 25 µm diameter wire held within two PMMA plates of 5mm and 10mm thick, see Figure 8a and 8b. The wire is stretched across a 10 mm thick, 240 x 300 mm PMMA plate. A 5 mm thick plate is then placed on top of this. The wire should be stretched (held under tension) until it is straight. Remove compression paddle. Position the MTF phantom (15 mm PMMA containing the wire) such that it is held 40 mm above the breast support platform. To measure the MTF in the chest wall-nipple direction, position the wire to run left-right across the detector at 60 mm from the chest wall edge. To measure the MTF in the tube-travel direction rotate the MTF phantom 90°, so the wire is centred left-right and is orthogonal to the tube-travel direction (at an angle). It is vital that the wire is held parallel to the detector and therefore remains within a given reconstructed plane. Take care that the phantom is not vibrating or moving as this will degrade the MTF. Set standard beam quality (typical target, filter, tube voltage and current–time product (mAs) for the standard test block) but no added filtration. Acquire a DBT scan and reconstruct using the reconstruction algorithm of interest (typical clinically used algorithm). Calculate in-plane MTF (left-right and front back) from the in-focus plane containing the wire using appropriate software. There may be some overshoot in the MTF, depending on the reconstruction algorithm used. Whereas for MTF measurements of projection images the MTF is normalized to MTF[0], for DBT it should be normalized to max(MTF). Re-bin to 0.25 mm^{-1} spatial frequency bins. Record spatial frequency for 50% and 10% points for the MTF.

Remark: system linearity and stationarity of statistics is assumed. The use of a small signal (thin wire) helps to fulfil this assumption, however this will not be fulfilled for non-linear reconstruction algorithms such as iterative methods. The usefulness of linear system theory metrics in DBT QC should be investigated further.

Remark: The contrast in the image of the MTF phantom should not be too high. Artefacts might be introduced which might influence the measurement.

Limiting values: Record spatial frequency for 50% and 10% points for the MTF. These values can be used for reference purposes and to ensure stability and similar settings/quality of the same type of system.
Frequency: Every six months
Equipment: 25 µm diameter W wire. Appropriate MTF calculation software.

5.4 Noise Power Spectra (optional)

See Appendix II.

5.5 Missed tissue

Missed tissue at chest wall side and at the top and bottom of the reconstructed tomosynthesis image is evaluated.

5.5.1 Missed tissue at chest wall side in the reconstructed tomosynthesis image

Method: Position two X-ray rulers on the bucky perpendicular to chest wall edge with a marker point at the bucky edge and acquire an image.

Evaluate the amount of missed tissue, i.e. the amount of tissue between the chest wall edge of the bucky and the chest wall edge of the reconstructed focal plane.

Instead of X-ray rulers, a phantom with markers can also be used.

Limiting values: Width of missed tissue at chest wall side ≤ 5 mm.
Frequency: Every six months
Equipment: X-ray rulers

5.5.2 Missed tissue at the top and bottom of the reconstructed tomosynthesis image

Method: Position some small high contrast objects (e.g. staples, paperclips) at the centre, near the chest wall edge and in each corner, on the bucky surface. Position the compression paddle at a height of 45 mm. Place some attenuating material between the bucky and compression paddle (for example 2 mm thick aluminium plate, or the standard test block) and acquire a tomosynthesis image under AEC control. Repeat the procedure with the high contrast objects taped to the underside of the compression paddle. use standard test block instead of aluminium and staples below and above. slight compression.

Check that all objects are brought into focus in focal planes near to the bottom and top of the reconstructed image, respectively.

Remark: take care not to scratch the bucky or compression paddle with the small high contrast objects.

Limiting values: All the objects at the bottom and top of the stack should be brought into focus within the reconstructed tomosynthesis image.

Frequency: Every six months
Equipment: Small high contrast objects, 2 mm thick aluminium plate

5.6 Homogeneity of the reconstructed tomosynthesis image

The evaluation of homogeneity is performed on the reconstructed tomosynthesis planes.

Method: Position a 45 mm thick PMMA block on the bucky covering the whole field of view and make an exposure in the clinically used AEC mode. Record the exposure factors. The focal planes of the reconstructed tomosynthesis image are divided in regions-of-interest (ROIs) of 5.0 mm by 5.0 mm. In each ROI the average pixel value, standard deviation and variance is calculated. Signal-to-noise ratio (SNR) is calculated for each ROI by dividing the average pixel value by the standard deviation. Calculate the average pixel value and SNR in the reference ROI. Also check all focal planes visually for artefacts and inhomogeneities.

Detector artefacts might be easier to evaluate on zero degree angle stationary mode or projection images. The method for evaluation of projection images is similar to FFDM.

Limiting values: No disturbing artefacts should be present. Record the pixel value and SNR in the reference ROI over time.
Frequency: Daily/Weekly
Equipment: Standard test block covering the whole field of view

5.7 Geometric distortion

Reconstructed planes of a phantom containing a rectangular array of 1mm diameter aluminium spheres or a similar set-up can be used to assess geometric distortion, see figure 9a.

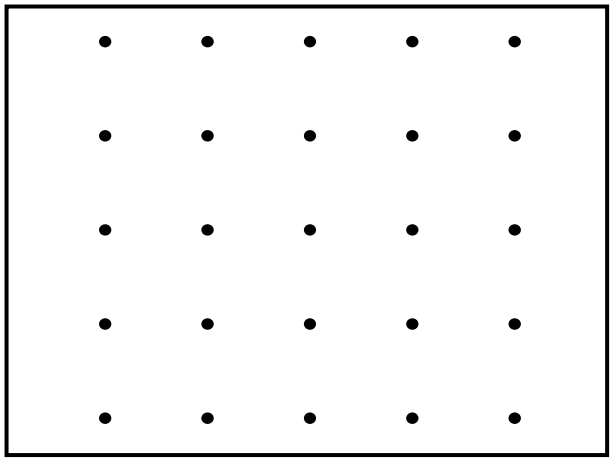

Figure 9a Example of a phantom for evaluation of geometric distortion; The phantom consists of a 5 mm thick PMMA slab with a rectangular array of 1mm diameter aluminium spheres embedded in the middle of the slab. The spheres are spaced at 55mm interval with an accuracy of +/-0.1mm.

Method: The geometric distortion phantom is imaged at the bottom, middle and top of a 60 mm stack of PMMA, see figure 9b and 9c.

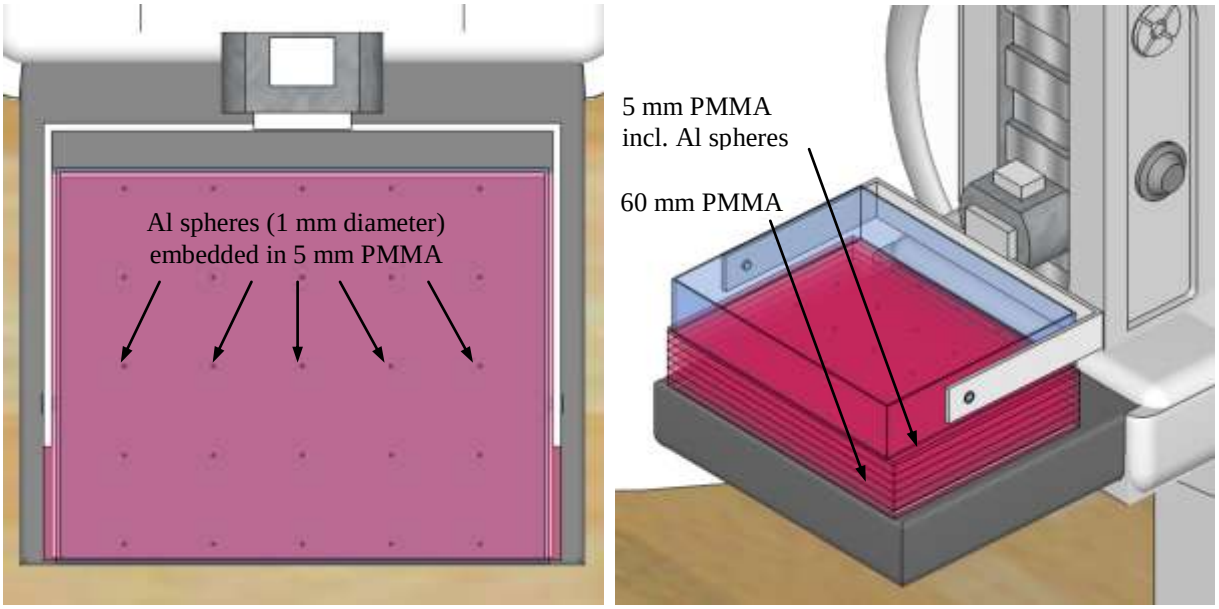

Figure 9b Setup for the evaluation of geometric distortion (60mm PMMA + 5mm phantom on top), top view and 3D-view.

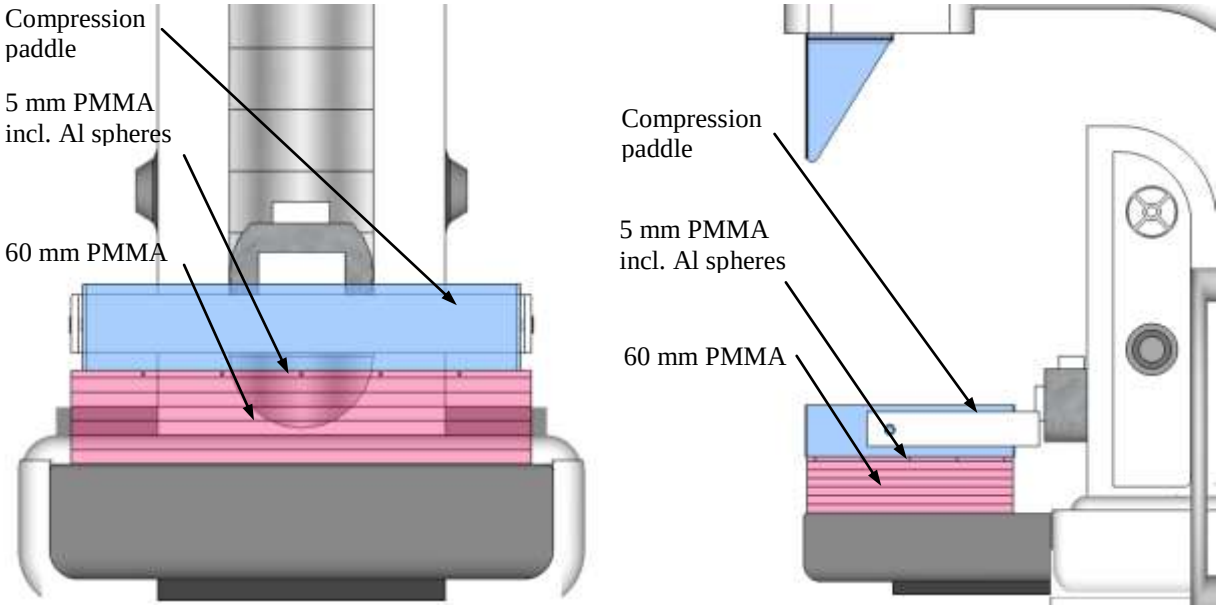

Figure 9c Setup for the evaluation of geometric distortion (60mm PMMA + 5mm phantom on top), front and side view.

Analysis software can be used to find the in focus position of each sphere in the x, y and z directions. This software will be made available via the EUREF website. This information can be used to assess whether the focal planes are flat (ie no distortion in the z direction), whether they

are tilted relative to the plane of the bucky surface, and to assess whether there is any distortion or inaccuracy of scaling within the focal planes.

Note: If it is found that the reconstructed focal planes are tilted relative to the surface of the breast support table, this information can be useful in determining how to position e.g. a CDMAM phantom such that the whole phantom is brought into focus within a single focal plane (section 5.1).

Limiting values:	Any distortion or scaling error should be within the manufacturer's specification. If the image has to be used for localisation purposes then the magnitude of any distortion or scaling error becomes important.
Frequency:	At acceptance
Equipment:	Phantom with rectangular array of aluminium spheres

6 Dosimetry for digital breast tomosynthesis

6.1 Introduction to DBT dosimetry

The procedures for estimating average glandular dose provided here for tomosynthesis systems are an extension to the procedure followed in 2D mammography and are described more fully in Dance *et al* 2011. A distinction is made between systems that have:

a full field detector and a X-ray tube that rotates above it so that the whole breast is irradiated in each exposure over a range of angles (full field geometry)

or

a narrow scanning beam which scans across the breast as the X-ray tube rotates, and for which the breast is only partially irradiated at each position of the X-ray tube (scanning geometry)

More information on both geometries is given in the Introduction.

In both tomographic geometries the conversion factors for determining the average glandular dose (AGD) were calculated for a breast compressed in the CC view, modelled as a cylinder of fixed semi-circular cross section but variable height. The radius of the breast was 80 mm and it comprised a central region which was a uniform mixture of adipose and glandular tissues surrounded on all sides apart from the chest wall by a 'shield region' of adipose tissue 5 mm thick, Dance et al (2011). The breast glandularity was defined as the fraction by weight of glandular tissue in the central region of the breast.

Tables 1 to 10 referred to below are given in appendix I.

6.1.1 Full field geometry

In breast tomosynthesis, the average glandular dose is the sum of the doses received from individual projections. For each projection angle θ equation (10) can be used to estimate the average glandular dose $D(\theta)$

$$D(\theta) = Kgcst(\theta) \qquad (10)$$

In this expression K is the incident air kerma at the top surface of the breast (without backscatter from the breast), **determined for the zero degree (straight through) position** using the current-time product (mAs) for angle θ. The quantities *g*, *c*, *s* and $t(\theta)$ are conversion factors. The factor *g* gives the AGD for a breast of glandularity 50% and is tabulated against breast thickness and HVL. The factor *c* allows for breasts of different glandularity and is tabulated against HVL and breast thickness for typical breast compositions. The factor *s* allows for the use of different X-ray spectra. Thus the first four quantities on the right hand side of the equation match the formalism used for dosimetry of conventional (2D) mammography introduced by Dance et al (2000) which is used in the European protocol. The final factor in the equation, $t(\theta)$, is the tomo factor for projection angle θ. Tabulations of the four factors are provided in Appendix I Tables 1-8. Data are given as a function of breast thickness and of PMMA thickness (for use when breasts are simulated with PMMA). The original publications of Dance (1990) and Dance et al (2000, 2009 and 2011) may be consulted for more information.

For a complete tomosynthesis examination the breast dose D_T can be found from

$$D_T = K_T g c s T \quad (11)$$

with

$$T = \sum_i \alpha_i t(\theta_i) \quad (12)$$

Here the summation is over all the projections off the tomosynthesis series and the α_i give the partition of the total current-time product (mAs) between the different projections. The incident air kerma K_T is measured in the 'zero degree' position, but is for the total current-time product of the tomosynthesis series. If the current-time product (mAs) for each projection is the same, the expression for T in equation (12) becomes:

$$T = \frac{1}{N} \sum_i t(\theta_i) \quad (13)$$

where N is the number of projections. With knowledge of the projection angles θ_i and the weights α_i the factor T can be calculated, using the data in appendix I Table 8. For a given tomosynthesis system using a fixed partition, this calculation only needs to be done once for each breast thickness. In calculating T, it is important to remember that the data in Appendix I Table 8 are tabulated as a function of the projection angle θ, not the tube rotation angle φ. The relationship between the two angles is:

$$\varphi = \theta + \sin^{-1}\left(\frac{d \sin\theta}{r}\right) \quad (14)$$

where r is the distance from the focal spot to the centre of rotation and d is the distance from the centre of rotation to the detector.

Appendix Table 9 gives values of T calculated from Appendix I Table 8 using equation (12) and is for use when the current-time-product (mAs) is the same for each projection and the angular increment between successive projections is the same. Appendix I Table 10 gives values of T which may be used for commercially available DBT systems. Updated versions of Appendix I Table 10 will be made available on the EUREF website as new equipment becomes available.

It should be noted that the actual geometry simulated in Dance *et al* (2011) had a radiation field matched to the image receptor size of 300x240 mm^2, the image receptor was 660 mm from the focal spot in the zero degree position, and the top of the breast support and the rotation axes were 15 mm and 40 mm respectively above the image receptor. As shown in the above paper, the values of $t(\theta)$ are insensitive to changes in the positions of the rotation axis and the focal spot receptor distance in the 'zero degree' position. Changes of ±40 mm in either of these parameters produced a change in $t(\theta)$ of 2.3% or less, with smaller changes in T.

6.1.2 Scanning geometry

The receptor of the currently available scanning breast tomosynthesis system has a reduced width (in this case 50 mm) and in order to image the whole breast, it rotates with the X-ray tube. For any given position of the X-ray tube only a small fraction of the breast is irradiated. The

relationship between the air kerma measured in the 'zero degree' position and the average glandular dose (D_S) is then sensitive to the beam width and the imaging geometry, and a slightly different formalism is therefore used.

In this case, normalisation is made to a measurement of air kerma made for a complete scanning movement. Equation (15) is used:

$$D_S = K_S g c s T_S \qquad (15)$$

Thus the tomo factor T_S is for a complete scanning movement and the air kerma K_S is determined for a complete scan of the system at the same current-time product (mAs) as the patient exposure, but without the breast.

The value of T_S is dependent on the position of the dose meter and the breast thickness and must be calculated separately for each scanning system geometry. Values of T_S are provided in Dance et al (2011) for measurements made with a dosimeter positioned on the upper surface of the breast support.

In summary the method of determining the AGD for the scanning tomosynthesis systems is the same as for fixed detector tomosynthesis systems except that

(a) Equation (15) is used

(b) The dose meter must be placed on the breast support table as the results are sensitive to the height of the dose meter above the breast support

(c) The incident air kerma K_s is determined using a full scan as for a patient examination rather than for a fixed 0º exposure

Appendix I Table 10 provides values of T_S for the Philips Microdose system.

6.2 Assessing Average Glandular Dose

6.2.1 Assessing AGD using the standard breast model simulated with PMMA

The doses to a range of typical breasts could be assessed using blocks of PMMA as breast substitutes and allowing the AEC to determine the exposure factors including any automatic selection of kV and target/filter combination and current-time product (mAs). This method relies on the equivalence in attenuation between different thicknesses of PMMA and typical breasts [Dance et al, 2000] as listed in Appendix 1 tables 1 and 2. It should be noted that since PMMA is denser than breast tissue any automatic selection of kV, target or filter may be slightly different from real breasts. This may be corrected by adding spacers (e.g. expanded polystyrene blocks) to the PMMA to make up a total thickness equal to the equivalent breast. Small pieces of more attenuating materials can also be used as spacers provided they are outside the sensitive area of the AEC. On systems that determine the exposure factors using transmission, spacers should not be necessary.

Set the AEC to the normally used clinical settings and expose PMMA slabs with total thickness of 20 mm. Record the exposure factors chosen by the AEC. Repeat for 30, 40, 45, 50, 60 and 70 mm PMMA thickness.

Calculate the average glandular dose to a typical breast of thickness and composition equivalent to the thickness of PMMA by applying equation 11 or 15 as appropriate. Note that the *c* and *g*-factors applied are those for the corresponding thickness of typical breast rather than the thickness of PMMA block used. Where necessary interpolation may be made for different values of HVL. Typical values of HVL for various spectra are given in Appendix I Table 3 but HVLs are normally measured at the same time as the measurements necessary to determine the incident air kerma. The factor *s* shown in Appendix I Table 4 corrects for any difference due to the choice of X-ray spectrum (Dance et al 2000, 2009 and 2011). For W/Al target/filter combinations the s-factor is tabulated against the thickness of breasts and PMMA. K (or K_S) is the incident air kerma (without backscatter) calculated **at the upper surface of the PMMA** using the method described below. Appendix I Table 10 gives values of T and T_S which may be used for commercially available DBT systems. Updated versions of Appendix I Table 10 will be made available on the EUREF website as new equipment becomes available.

The determination of incident air kerma at the surface of PMMA test phantoms should be based on measurements made with a geometry which includes scatter from the paddle. It is advisable to place a thin steel plate on the breast support to fully cover the imaging detector to prevent ghost images of the dosimeter in subsequent images.

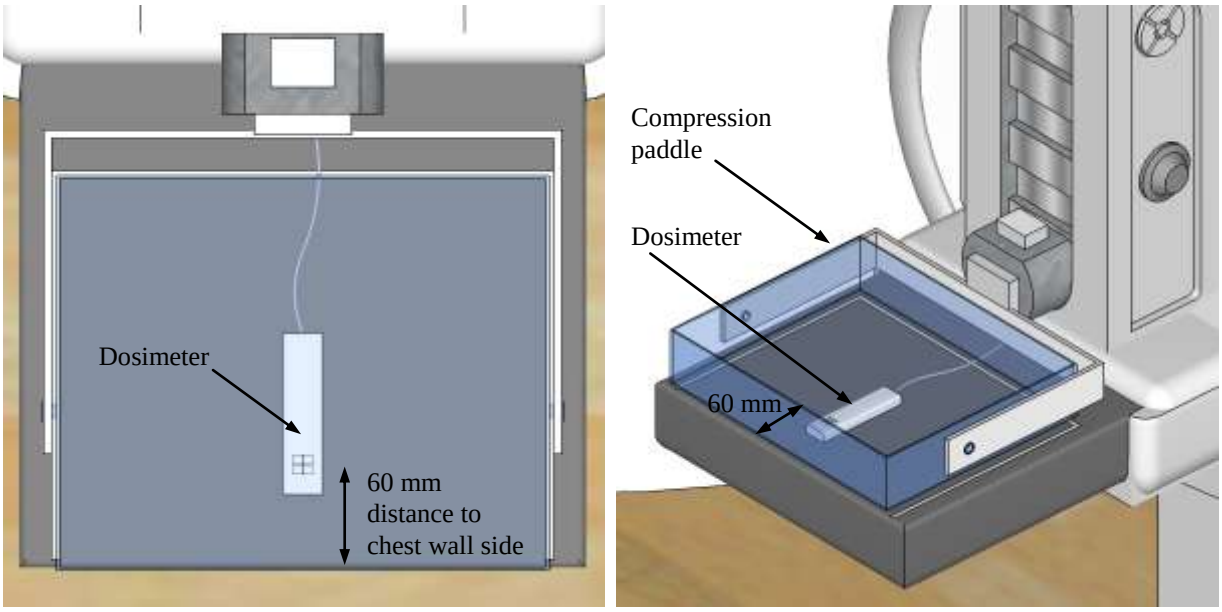

Figure 10a Position of dosimeter to determine the incident air kerma for dose estimation, top view and 3D-view.

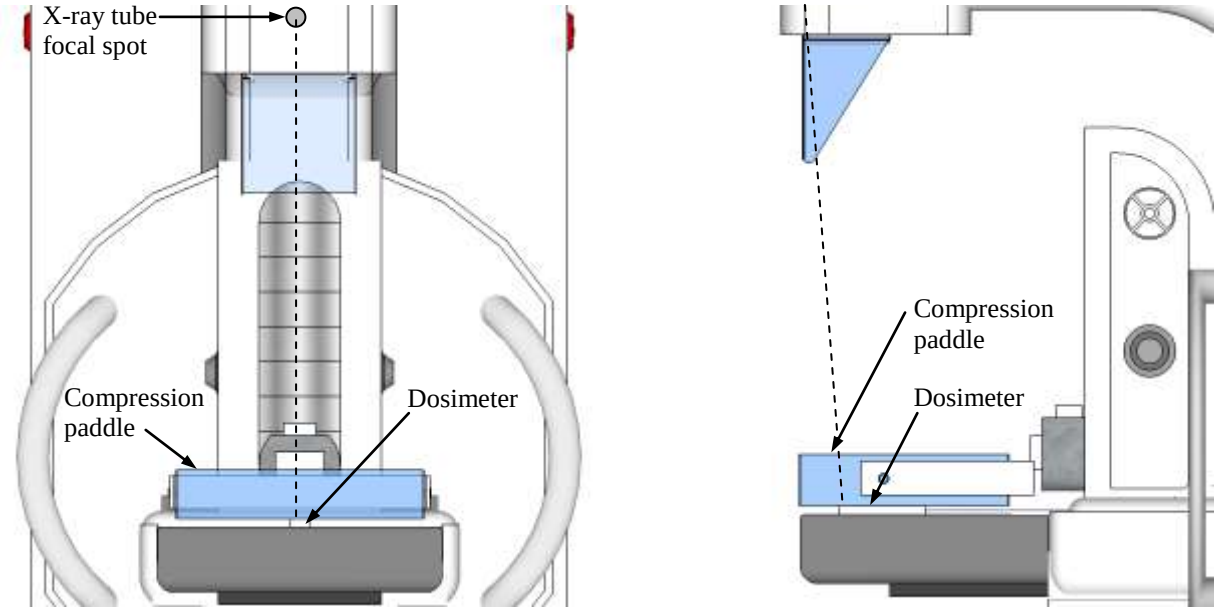

Figure 10b Position of dosimeter to determine the incident air kerma for dose estimation, front and side view.

The dose meter should be positioned on a line extending from the tube focal spot to a point on the mid-line of the breast support table 60 mm from the chest wall edge. If the dose meter has back scatter correction, the recommended position for a full field imaging geometry is directly on the breast support (or the steel sheet covering it – see above) with the paddle in contact (Figure 10). For a scanning geometry, this position is mandatory (see above), and if necessary a correction for backscatter would need to be applied. For a full field imaging geometry, it would also be possible to make a measurement of air kerma with the dosimeter higher above the breast support and with the paddle in contact provided appropriate inverse square law correction is made. This approach is recommended if the dose meter does not have backscatter correction. The effect of scatter from the compression paddle on the measurement of incident air kerma is discussed in Dance et al 2009 where it is shown that for the above geometry, and a polycarbonate paddle of 2.4 mm thickness scattered photons contribute 7% of the total measured air kerma. For some designs of dosimeter, a small correction to the dosimeter reading may be necessary because of variation of the dosimeter response with angle.

Calculate the incident air kerma for each of the beam qualities used in exposing the blocks of PMMA by making an exposure of the dosimeter positioned as discussed above using a manually selected current-time product (e.g. 50 mAs) and the tube fixed at the ‘zero degree’ position. Estimate the incident air kerma at the upper surface of the PMMA by using the inverse square law and scaling to the appropriate value of current-time product (mAs).

6.2.2 Assessing clinical breast doses

It is also possible to measure the average glandular dose for a series of breast examinations on each mammography system. To do this, for each exposure the breast thickness under compression is measured, and the exposure factors are recorded. From measurements of air kerma as described above at the tube voltage and target/filter combination used, the current-time product (mAs) may be used to estimate the incident air kerma and to determine the average glandular dose using equations 11 or 15 as appropriate. In this case the incident air kerma K (or K_S) is calculated at the upper surface of the breast. g-factors should be interpolated for the appropriate breast thickness from Appendix I Table 5. c-factors for typical breast compositions in the age ranges 50 to 64 years and 40 to 49 years are shown in Appendix I Tables 6 and 7. The compressed thickness on the X-ray set should be recorded. The accuracy of the displayed thickness should be verified by applying a typical force (e.g. 100 N) to a block of compressible foam (dimensions 180mm x 240mm) in which a strip has been cut out to allow measurement of compressed thickness, see figure 11. Record the thickness indication and measure thickness at the reference point with an appropriate device (for example a ruler). Perform this measurement of several blocks of foam such that the thicknesses from 20 to 100 mm can be verified

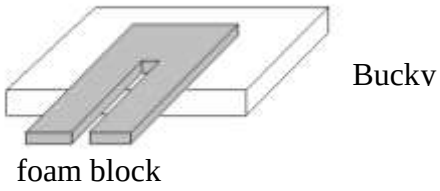

Fig. 11 The position of the foam block on the bucky

It may be necessary to apply correction factors if the displayed values are in error. An accuracy of ± 2 mm is required (Faulkner and Cranley, 2005). Appendix I Table 10 gives values of T and T_S which may be used for commercially available DBT systems. Updated versions of Appendix I Table 10 will be made available on the EUREF website as new equipment becomes available.

The data in Appendix I Tables 9-11 have been calculated for a standard breast model examined in the CC-view. The values of $t(\theta)$ for the MLO view are quite different (Sechopoulos *et al*, 2007), but after integration, the resulting values of T for MLO and CC views are similar, and provided the weights for each projection angle are the same, for practical purposes, the T-factors for the CC-projection can be used (Dance et al, 2011).

Reference value: To be determined. It is advised to use the limiting values of the European Guidelines as reference value, see table 3.

Table 3 Reference values for AGD at different thicknesses for tomosynthesis X-ray units or tomosynthesis mode on mammographic X-ray units (if FFDM imaging is possible).

Thickness of PMMA	Equivalent breast thickness	Average glandular dose to equivalent breasts
		Reference level level
(mm)	(mm)	(mGy)
20	21	1.0
30	32	1.5
40	45	2.0
45	53	2.5
50	60	3.0
60	75	4.5
70	90	6.5

Frequency: Every six months
Equipment: Suitable dose meter, blocks of foam of several thicknesses

7 Image presentation

The tests in this section are based upon the work of AAPM TG18 (American Association of Physicists in Medicine, Task Group 18). The TG18 test patterns described in this section should be downloaded from the TG18 website (2k versions should be used when available): http://deckard.mc.duke.edu/~samei/tg18. Some mammography display systems need adjusted versions of the test patterns, these are available from the EUREF website.

Some general remarks:
- The test patterns have to be displayed at full resolution (exactly one display pixel for each pixel in the digital image) or printed at full size; contrast and brightness of the images may not be adjusted.
- Some of the tests in this chapter are for Cathode Ray Tube (CRT) displays or Liquid Crystal Displays (LCDs) only.
- A magnifying glass may be used in the evaluation of printed images
- The monitors should be tested as used clinically (e.g. third monitor on, viewing boxes on covered with films)

7.1 Monitors

7.1.1 Ambient light

Most of the quality tests in this chapter are highly sensitive to ambient light, therefore all of them should be performed under clinical conditions (room lights, light boxes and other display devices should be at the same luminance level as under clinical conditions). The ambient light should be measured at the centre of the display with the light detector facing outwards and the display switched off.

Limiting value	*Ambient light should be less than 20 lux for primary display devices. [The maximum ambient light actually depends on the reflection characteristics and minimum luminance of the monitor, but for reasons of simplicity this is ignored here.]*
Frequency	*Every six months.*
Equipment	*Illuminance meter*

7.1.2 Geometrical distortion (CRT displays)

Visually check whether the TG18-QC image (figure 12) is displayed without geometrical distortion. To do so, inspect the lines and borders of the test pattern.

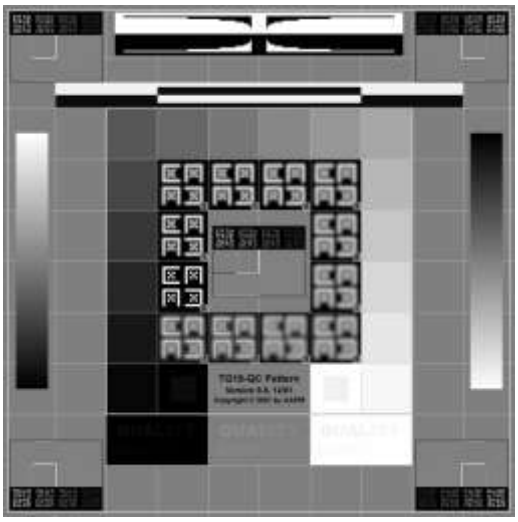

Figure 12 TG18-QC test pattern

Limiting value	*Borders should be completely visible, lines should be straight, the active display area should be centred on the screen*
Frequency	*Daily*
Equipment	*TG18-QC test pattern*

7.1.3 Contrast visibility

The TG18-QC test pattern contains several items for evaluating the contrast visibility of a display.
Each of the sixteen luminance patches, located approximately equidistant from the centre of the image, contains four corner squares at equal low contrast steps to the patch (figure 13). The two patches in the bottom with minimum and maximum pixel value, surrounding the test pattern name, contain a centre square with a pixel value of 5% and 95% of the maximal grey level respectively. The letters “QUALITY CONTROL” in the three rectangles below these patches are displayed with decreasing contrast to the background. The visible part of the letters should be written down and checked with the visibility at acceptance, in order to keep track of contrast degradation. If contrast visibility is not sufficient, it may help to dim the room lights. If this is done however, the lights should also be dimmed while using the displaying system clinically. The appearance of the TG18-QC test pattern also depends on the mapping of pixel values to luminance. Therefore if this test has failed, the tests in sections 7.1.6 and 7.1.7 should be performed.

Remark: It should be kept in mind that the luminance of LCD monitors depends on the viewing angle. When large viewing angles are used, contrast visibility may not comply with the limiting values.

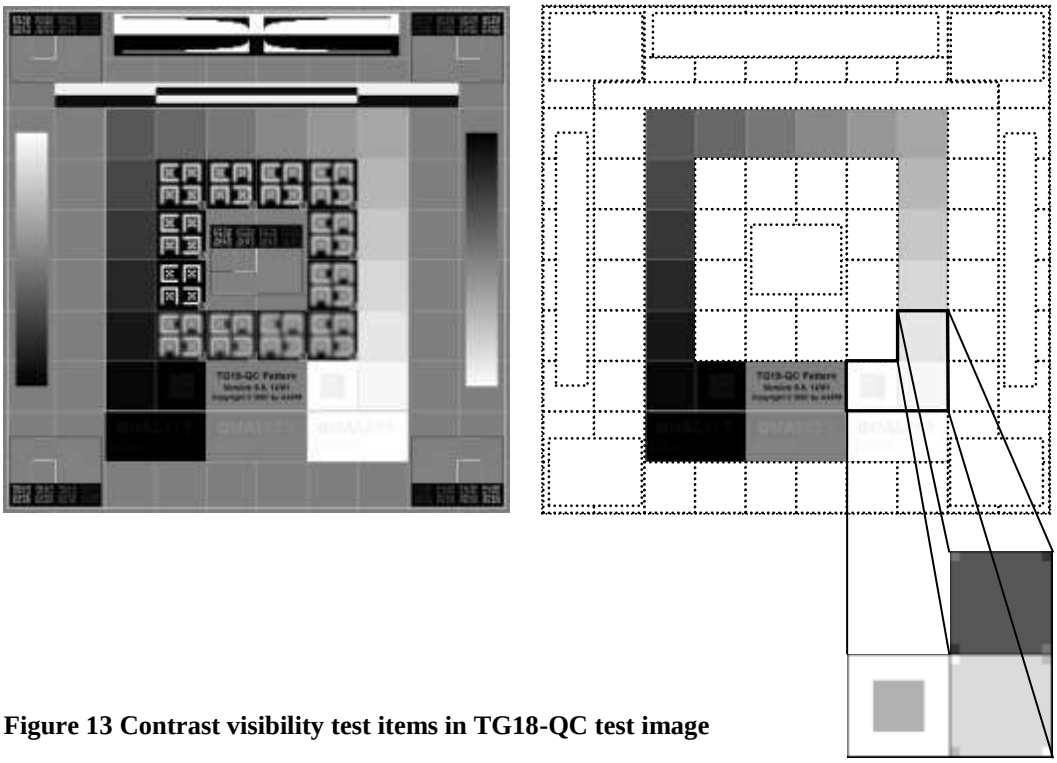

Figure 13 Contrast visibility test items in TG18-QC test image

Limiting value	*All corner patches should be visible, the 5% and 95% pixel value squares should be clearly visible*
Frequency	*Daily*
Equipment	*TG18-QC test pattern*

7.1.4 Resolution

Evaluate horizontal and vertical line patterns to check display resolution visually.
AAPM Task Group 18 provides 6 line patterns at different background luminance levels. (Horizontal line patterns TG18-LPH10, -LPH50 and –LPH89; Vertical line patterns TG18-LPV10, -LPV50 and –LPV89.)

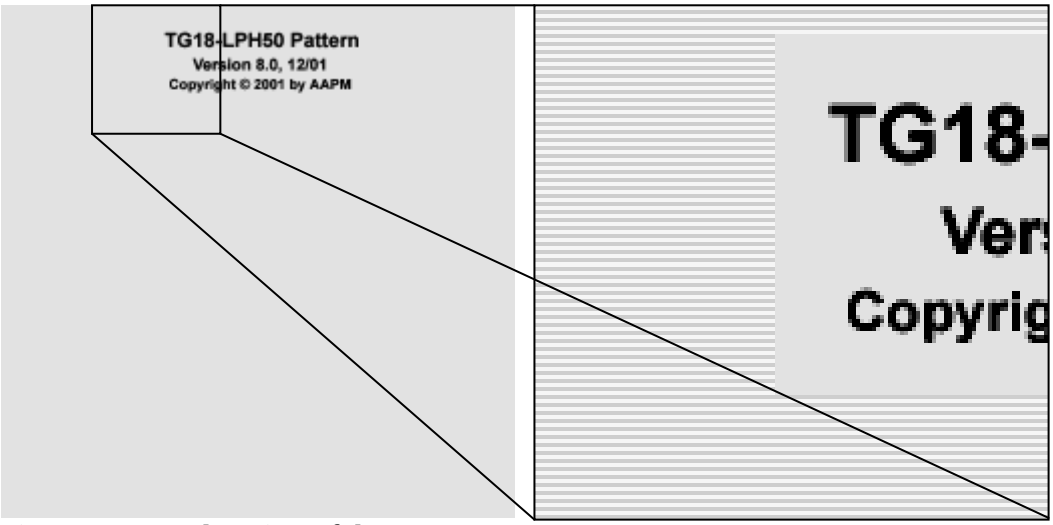

Figure 14 Zoomed versions of the TG18-LPH50 pattern

Limiting value	*All line patterns should be discernible*
Frequency	*Every 6 months*
Equipment	*2kx2k TG18-LPH10, TG18-LPH50, TG18-LPH89, TG18-LPV10, TG18-LPV50 and TG18-LPV89 test patterns*

7.1.5 Display artefacts

The TG18-QC test pattern also contains some elements, which can be used for recognising display artefacts. The image should be carefully checked for defect pixels (LCD only), steps in the black-to-white and white-to-black ramp bars (this can reveal an insufficient bit depth), and artefacts near the black-to-white and white-to-black transitions (video card). Also pay attention to temporal instability (flicker) and spatial instability (jitter).

Limiting Values	*No disturbing artefacts should be visible*
Frequency	*Daily*
Equipment	*2kx2k TG18-QC test pattern*

7.1.6 Luminance range

Measure the maximum and minimum luminance of the display device. Test patterns TG18-LN12-01 and TG18-LN12-18 can be used.
The ratio of maximum and minimum display luminance, in the presence of ambient light, is an indicator of luminance contrast response capabilities of the monitor (under the current environmental conditions). Both luminances should be measured using a telescopic luminance meter, to include the influence of ambient light.
DICOM GSDF conformance (section 4.1.7) makes sure the available contrast is spread out in an appropriate and standard manner over the full greyscale range of the monitor.

Remark: It should be kept in mind that the luminance of LCD monitors depends on the viewing angle. When large viewing angles are used, the luminance range may not comply with the limiting values.

Limiting Values	*The maximum to minimum luminance ratio should be at least 350 for primary display devices[1], or 100 for secondary display devices. The maximum luminance should exceed 500 cd/m^2. The difference of maximum luminances between displays belonging to one displaying station should not exceed 5% of the lowest.*
Frequency	*Every six months or when contrast visibility has changed*
Equipment	*Telescopic luminance meter, TG18-LN12-01 and TG18-LN12-18 test patterns*

7.1.7 Greyscale Display Function

To make sure a mammogram will appear similarly on different viewing stations and on printed film, the mapping of greyscale values to display luminance or optical density should be consistent. In this measurement it is determined whether a display conforms to the DICOM Greyscale Standard Display Function (GSDF).

The greyscale display function (GDF) can be determined by measuring the luminance of the 18 AAPM luminance test patterns (TG18-LN12-01 through TG18-LN12-18). The test patterns should be displayed full screen and the luminance has to be measured at the centre of the screen. The shape of the GDF depends on the ambient light in the room. Therefore room lights, light boxes and other display devices should be at the same luminance level as when the system is used clinically. A telescopic luminance meter should be used to include the influence of ambient light.

The measured values can be inserted into a spreadsheet (available on the Euref website: www.euref.org) to automatically determine GSDF conformance.

[1] Note that the limiting value for this maximum to minimum luminance ratio has been changed compared to the fourth edition of the Guidelines.

Remark: This test only applies to primary and secondary display systems. The acquisition workstation monitor is excluded from this test. This monitor should only be used to check positioning techniques, not for diagnosis and image quality checks.

Remark: It should be kept in mind that the luminance of LCD monitors depends on the viewing angle. When large viewing angles are used, the display on a monitor may not comply with the GSDF.

Limiting value	*The calculated contrast response should fall within ± 10% of the GSDF contrast response for primary class displays (± 20% for secondary class displays)*
Frequency	*Every six months and when contrast visibility has changed*
Equipment	*Telescopic luminance meter, TG18-LN12-01 through TG18-LN12-18 test patterns*

7.1.8 Luminance uniformity

When the display has been tested for DICOM conformance at the centre of the monitor, this does not mean contrast visibility is optimal at every position on the monitor. One could test the GDF for several locations on the monitor, but it is more convenient to check display uniformity. Measure the display luminance at five locations for each monitor. The test patterns TG18-UNL10 and TG18-UNL80 can be used (figure 15).

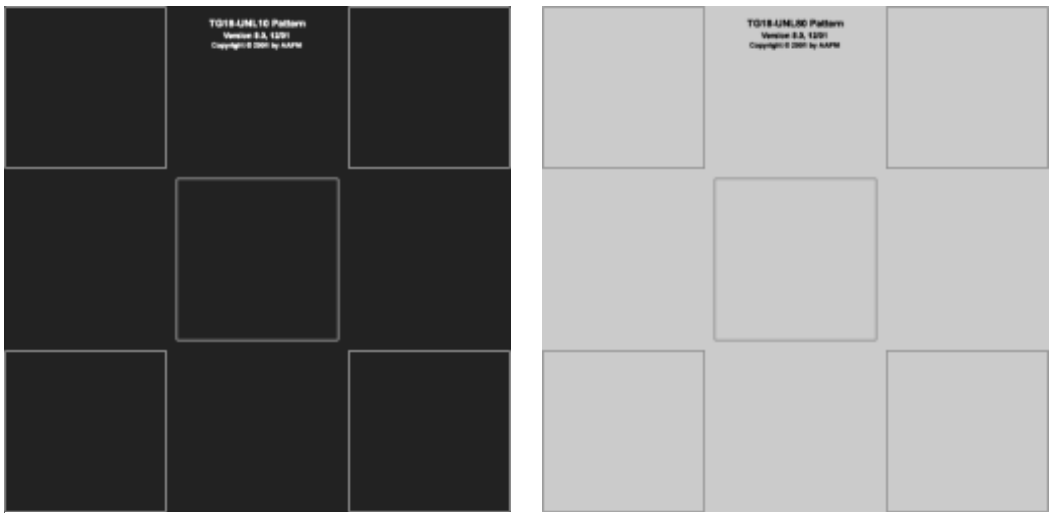

Figure 15 TG18-UNL10 and TG18-UNL80

Limiting value	*Maximum luminance deviation of a display device should be less than 30% ((Lmax-Lmin)/Lcentre<0.3).*
Frequency	*Every six months and when contrast visibility has changed*
Equipment	*Luminance meter (telescopic luminance meters should be equipped with a cone or baffle for this measurement), TG18-UNL10 and TG18-UNL80 test patterns*

2b.4.1.2 - 5 Alternative: Constancy test of monitor performance

In the following section we describe alternative test patterns that allow to test contrast visibility, distortion and artefacts as efficient as with the AAPM test patterns. The so-called 'MoniQA' pattern is one such example (Jacobs 2007). The complete procedure includes the generation of an always new test pattern at every evaluation and a fill-in sheet of which the readings are compared to the truth. This overcomes inattentive scorings and allows an easy verification of adherence to the Quality Control procedures. The software to create and score the test patterns is downloadable via the EUREF website.

The pattern is divided in four equally sized, rectangular segments with four uniform background values of different intensities. The values were chosen to be 0%, 33%, 66% and 100% of the maximum gray level. The position of these rectangles swaps randomly each time the pattern is generated with one restriction: the rectangle with a gray level of 0% (L_{min}) will always have a mutual border with the rectangle with a gray level of 100% (L_{max}). This guarantees the creation of a black-to-white or white-to-black transition between the patches with the highest and the lowest gray level. This transition can be either horizontal or vertical. Figure 16 shows two examples of the variable pattern.

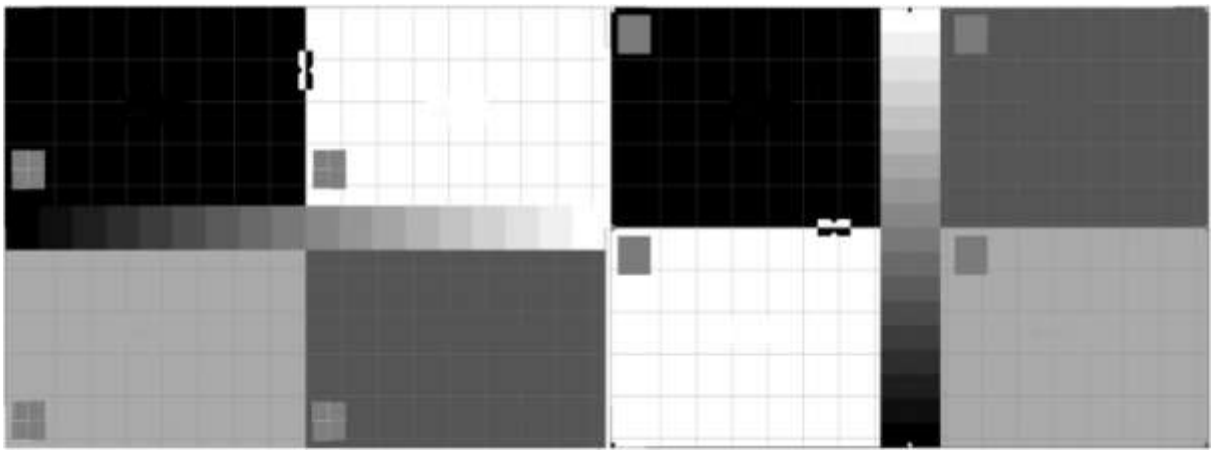

Figure 16 Two examples of the MoniQA pattern. These patterns include checks for contrast visibility, geometric distortion, spatial resolution, global image quality and artifacts. (reprinted with permission from *Med Phys*)

Extra tests:

(a) Low contrast characters

Protocol for the Quality Control of the Physical and Technical Aspects of Digital Breast Tomosynthesis systems, version 1.0

In the center of each rectangular segment there is a set of five characters that creates a low contrast with the background pixel value (Figure 17a). Each time the pattern is created the characters are randomly chosen out of a subset of the Latin alphabet, namely *ABCDEHJKLMPSTUZ*. Each set of characters has pixel value differences of 7, 5, 3, 2 and 1 between background and character. The observer has to read as many characters as possible. We suggest that the observer guesses the value of one character more than what he readily sees.

Score criteria: If characters are not discriminated from the background, points are subtracted from the initial score of 100 according to the pixel value difference between character and background. If the least visible character is not read, 1 point is deducted. The next character has a value of two points; the third character has a value of three points. For the fourth character, 5 points are deducted and if the highest contrast character is not detectable 7 points are deducted.

(b) Gradient bar of patches with increasing pixel values and low contrast characters
In the center of the display, a gradient bar of 18 distinct grayscale steps is drawn, with pixel values as used in the central rectangle of the AAPMtg18-LN patterns. This bar is horizontal or vertical but will never divide the rectangles with 0% and 100% of the maximum gray level. A random character is placed on each step of the gradient. The bar is divided in 2 equally sized parts, a northern and southern part or a western and eastern part. In each part of the gradient bar, each character is unique. For the selection of the characters, we use the same alphabet as used for the selection of the low contrast characters. The grayscale value of each character is the same as the grayscale value of the preceding luminance patch (Figure 17b), with the whitest and darkest patches at the extremes.

To evaluate this pattern, characters are to be read, starting in the middle and according to the orientation of the bar, towards West, East, North and South. If a luminance character is visible, we conclude that the underlying patch can be clearly distinguished from the adjacent patch. In the AAPMtg18-QC and the DIN test pattern, the purpose of this gradient bar is to verify whether the different steps are distinguishable. This is most critical for the lowest and highest pixel values. When evaluating the MoniQA pattern, only the two last visible characters have to be registered.

Score criteria: 10 points are deducted for each incorrectly identified or invisible low luminance patch and this for both extremities of the gradient bar. If no character has been filled in, 9 times 10 points are deducted.

(c) The MoniQA pattern allows to test geometric distortion, the fact whether all pixels of the test image are shown, high and low contrast spatial resolution, and artefacts (black-to-white and white-to-black transition problems. Any defects lower the score with 5 points, except a dead pixel that lowers the score with 11 points.

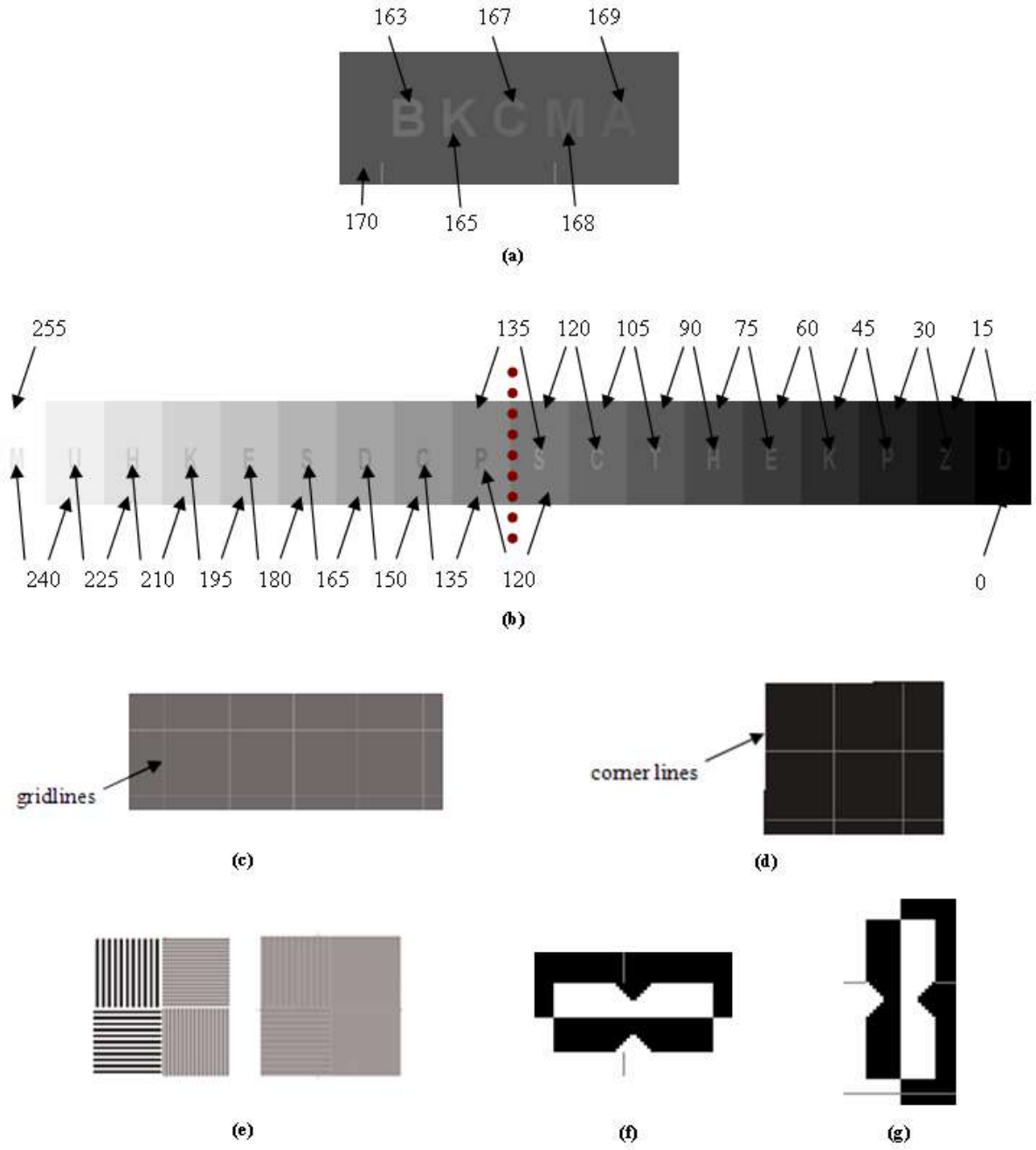

Figure 17 – (a) example of a sequence of characters with a low contrast luminance difference with the background – (b) gradient bar of patches with decreasing pixel values and with random characters having a pixel value as in the adjacent patch – (c) grid pattern – (d) corner lines pattern – (e) resolution patterns, left: high contrast, right: low contrast – (f) and (g) horizontal and vertical version of the hourglass object

(all elements are shown with enhanced contrast for clarity)

The MoniQA pattern is variable. There are 16 combinations of background positions, 4 positions for the resolution pattern inside each background field and 2 resolution types (high and low contrast) which makes a total number of 128 possible configurations. In addition, there is a very large number of combinations of characters for the low contrast visibility checks.

Limiting value	Score retrieved from MoniQA pattern should be higher or equal to 95
Frequency	Daily, optional weekly
Equipment	MoniQA test pattern

References

Boone JM, Fewell TR, Jennings RJ, Molybdenum, rhodium, and tungsten anode spectral models using interpolating polynomials with application to mammography, *Med.Phys.*, vol. 24 (1997) 1863-1874

Bouwman R, Young K, Lazzari B, Ravaglia V, Broeders B, van Engen R, An alternative method for noise analysis using pixel variance as part of quality control procedures on digital mammography systems, *Phys Med Biol*. 54 (2009) 6809-6823

Bouwman RW, Visser R, Young KC, Dance DR, Lazzari B, van der Burght R, Heid P, van Engen RE, Daily quality control for breast tomosynthesis, *Proceedings of SPIE Medical Imaging* 2010

Bouwman RW, Diaz O, Young KC, van Engen RE, Veldkamp WJH, Dance DR, Phantoms for quality control procedures of digital breast tomosynthesis, in: Maidment (ed), *Breast Imaging, proceedings* IWDM 2012 322-329

Bouwman RW, Diaz O, van Engen RE, Young KC, den Heeten GJ, Broeders MJM, Veldkamp WJH, Dance DR, Phantoms for quality control procedures in digital breast tomosynthesis: dose assessment, in: *Phys Med Biol* 58 (2013) 4423–4438

Byng JW, Mainprize JG, Yaffe MJ, 1998, X-ray characterization of breast phantom materials, *Phys.Med.Biol.*, vol. 43 (1998) 1367-1377

Dance DR Monte Carlo calculation of conversion factors for the estimation of mean glandular breast dose. *Phys. Med. Biol.* 35 (1990) 1211-1219

Dance DR, Skinner CL, Young KC, Beckett JR, Kotre CJ, Additional factors for the estimation of mean glandular breast dose using the UK mammography dosimetry protocol *Phys.Med. Biol.* 45 (2000) 3225-3240

Dance DR, Young KC, van Engen RE, Further factors for the estimation of mean glandular dose using the United Kingdom, European and IAEA dosimetry protocols. *Phys. Med. Biol.* 54 (2009) 4361-72

Dance DR, Young KC, van Engen RE, Estimation of mean glandular dose for breast tomosynthesis: factors for use with the UK, European and IAEA breast dosimetry protocols. *Phys. Med. Biol.* 56 (2011) 453-471

Dobbins JT, Tomosynthesis imaging: At a translational crossroads, *Med. Phys.* 36 (2009) 1956-1967

Faulkner K, Cranley K, An investigation into variations in the estimation of mean glandular dose in mammography. *Rad. Prot. Dosim.* 57 (1995) 405-408

Hsieh J, Computed Tomography second edition, SPIE publications 2009

IEC 62220-1-2, Medical Electrical Equipment –Characteristics of digital X-ray imaging Devices, Part 1: Determination of the detective quantum efficiency

Jacobs J, Marshall N, Cockmartin L, Zanca F, van Engen R, Young K, Bosmans H, Samei E, Towards an international consensus strategy for periodic quality control of digital breast tomosynthesis systems, in: Hsieh J, Samei E (ed), *Proceedings SPIE Medical Imaging 2010: The Physics of Medical Imaging*

Johns PC, Yaffe MJ, X-ray characterisation of normal and neoplastic breast tissues *Phys.Med.Biol.*, vol. 32 (1987) 675-695

Marshall NW, Jacobs J, Cockmartin L and Bosmans H 2010 Technical evaluation of a digital breast tomosynthesis system LNCS 6136, 350–356 in Martí J et al. (Eds.) *Proceedings IWDM 2010*

Marshall NW, Bosmans H. Measurements of system sharpness for two digital breast tomosynthesis systems, *Phys. Med. Biol*. 2012 57 (2012) 7629-50.

Monnin P, Bosmans H, Verdun FR, Marshall NW, Comparison of the polynomial model against explicit measurements of noise components for different mammography systems, *Phys Med Biol.* 59 (2014) 5741-61

Perry N et al (ed.), European Guidelines for quality assurance in breast cancer screening and diagnosis, fourth edition, European Commission, 2006

Sechopoulos I, Suryanarayanan S, Vedantham S, Karellas A, D'Orsi CJ, Computation of the glandular radiation dose in tomosynthesis of the breast. *Med. Phys*. 34 (2007) 221-232

Sechopoulos I, A review of breast tomosynthesis. Part I. The image acquisition process, *Med. Phys.* 40 (2013) 014301

Sechopoulos I, A review of breast tomosynthesis. Part II. Image reconstruction, processing and analysis, and advanced applications, *Med Phys*. 40 (2013) 014302

Siewerdsen JH, Cunningham IA and Jaffray DA A framework for noise-power spectrum analysis of multidimensional images *Med. Phys.* 29 (2002), 2655-2671

van Engen R, Bouwman R, van der Burght R, Lazzari B, Dance D, Heid P, Aslund M, Young K, Image quality measurements in breast tomosynthesis, in: Krupinski (ed), *Digital mammography, 2008*, 696-702

Young KC, Cook JJH, Oduko JM, Bosmans H, Comparison of software and human observers in reading images of the CDMAM test object to assess digital mammography systems. In: Flynn MJ, Hsieh J (eds): *Proceedings of SPIE Medical Imaging 2006*, 614206 (2006) 1-13.

Young KC, Oduko JM, Bosmans H, Nijs K, Martinez L, Optimal beam quality selection in digital mammography, *British Journal of Radiology* 79 (2006), 981-990

Zhao B, Zhou J, Hu Y-H, Mertelmeier T, Ludwig J, Zhao W, Experimental validation of a three-dimensional linear system model for breast tomosynthesis *Med. Phys.* 36 (2008) 240-251

Zhao B, Zhao W, Three-dimensional linear system analysis for breast tomosynthesis *Med. Phys.* 35 (2008)5129-5232

Zhou J, Zhao B and Zhao W, A computer simulation platform for the optimization of a breast tomosynthesis system *Med. Phys.* 34 (2007) 1098-1109

Appendix I. Tables for dosimetry calculation in digital breast tomosynthesis

Table 1 g-factors for breasts simulated with PMMA

PMMA thickness (mm)	Equiv. breast thickness (mm)	Gland. of equiv. breast (%)	g-factors (mGy/mGy)										
			HVL (mm Al)										
			0.30	0.35	0.40	0.45	0.50	0.55	0.60	0.65	0.70	0.75	0.80
20	21	97	0.378	0.421	0.460	0.496	0.529	0.559	0.585	0.609	0.631	0.650	0.669
30	32	67	0.261	0.294	0.326	0.357	0.388	0.419	0.448	0.473	0.495	0.516	0.536
40	45	41	0.183	0.208	0.232	0.258	0.285	0.311	0.339	0.366	0.387	0.406	0.425
45	53	29	0.155	0.177	0.198	0.220	0.245	0.272	0.295	0.317	0.336	0.354	0.372
50	60	20	0.135	0.154	0.172	0.192	0.214	0.236	0.261	0.282	0.300	0.317	0.333
60	75	9	0.106	0.121	0.136	0.152	0.166	0.189	0.210	0.228	0.243	0.257	0.272
70	90	4	0.086	0.098	0.111	0.123	0.136	0.154	0.172	0.188	0.202	0.214	0.227
80	103	3	0.074	0.085	0.096	0.106	0.117	0.133	0.149	0.163	0.176	0.187	0.199

Table 2 c-factors for breasts simulated with PMMA

PMMA thickness (mm)	Equiv. breast thickness (mm)	Gland.of equiv. breast (%)	c-factors										
			HVL (mm Al)										
			0.30	0.35	0.40	0.45	0.50	0.55	0.60	0.65	0.70	0.75	0.80
20	21	97	0.889	0.895	0.903	0.908	0.912	0.917	0.921	0.924	0.928	0.933	0.937
30	32	67	0.940	0.943	0.945	0.946	0.949	0.952	0.953	0.956	0.959	0.961	0.964
40	45	41	1.043	1.041	1.040	1.039	1.037	1.035	1.034	1.032	1.030	1.028	1.026
45	53	29	1.109	1.105	1.102	1.099	1.096	1.091	1.088	1.082	1.078	1.073	1.068
50	60	20	1.164	1.160	1.151	1.150	1.144	1.139	1.134	1.124	1.117	1.111	1.103
60	75	9	1.254	1.245	1.235	1.231	1.225	1.217	1.207	1.196	1.186	1.175	1.164
70	90	4	1.299	1.292	1.282	1.275	1.270	1.260	1.249	1.236	1.225	1.213	1.200
80	103	3	1.307	1.299	1.292	1.287	1.283	1.273	1.262	1.249	1.238	1.226	1.213

Table 3 Typical HVL measurements for different tube voltage and target filter combinations. (Data includes the effect on measured HVL of attenuation by a compression paddle.)

	HVL (mm Al) for target filter combination						
kV	Mo Mo	Mo Rh	Rh Rh	W Rh	W Ag	W Al (0.5mm)	W Al (0.7mm)
25	0.32 ± .02	0.38 ± .02	0.37 ± .02	0.50 ± .03	0.51 ± .03	0.34 ± .03	0.42 ± .03
28	0.35 ± .02	0.42 ± .02	0.42 ± .02	0.53 ± .03	0.58 ± .03	0.39 ± .03	0.49 ± .03
31	0.38 ± .02	0.45 ± .02	0.45 ± .02	0.56 ± .03	0.61 ± .03	0.44 ± .03	0.55 ± .03
34	0.40 ± .02	0.47 ± .02	0.47 ± .02	0.59 ± .03	0.64 ± .03	0.49 ± .03	0.61 ± .03
37				0.62 ± .03	0.67 ± .03	0.53 ± .03	0.66 ± .03

Table 4a s-factors for clinically used spectra [Dance et al 2000, 2009, 2011].

Target material	Filter material	Filter thickness (μm)	s-factors
Mo	Mo	30	1.000
Mo	Rh	25	1.017
Rh	Rh	25	1.061
W	Rh	50-60	1.042
W	Ag	50-75	1.042

Table 4b s-factors for a tungsten target filtered by 0.5 mm aluminium [Dance et al 2000, 2009, 2011].

PMMA thickness (mm)	Equiv breast thickness (mm)	s-factor
20	21	1.075
30	32	1.104
40	45	1.134
45	53	1.149
50	60	1.160
60	75	1.181
70	90	1.198
80	103	1.208

Table 4c s-factors for a tungsten target filtered by 0.7 mm aluminium. This table is an extension of the data published in Dance et al 2000, 2009, 2011.

PMMA thickness (mm)	Equiv breast thickness (mm)	s-factor
20	21	1.052
30	32	1.064
40	45	1.082
45	53	1.094
50	60	1.105
60	75	1.123
70	90	1.136
80	103	1.142

Table 4d s-factors for a tungsten target filtered by 0.5 mm aluminium[Dance et al 2000, 2009, 2011].

Breast thickness (mm)	Glandularity range (%)	Typical glandularity age 50-64	Typical glandularity age 40-49	kV range (kV)	s-factor
20	80-100	100	100	25-40	1.069
30	62-82	72	82	29-40	1.104
40	40-65	50	65	29-40	1.127
50	23-49	33	49	30-40	1.139
60	11-35	21	35	30-40	1.154
70	2-24	12	24	30-40	1.180
80	0.1-17	7	14	30-40	1.187
90	0.1-14	4	8	30-40	1.198
100	0.1-13	3	5	30-40	1.206
110	0.1-13	3	5	30-40	1.212

Table 4e s-factors for a tungsten target filtered by 0.7 mm aluminium.

Breast thickness (mm)	Glandularity range (%)	Typical glandularity age 50-64	Typical glandularity age 40-49	kV range (kV)	*s*-factor
20	80-100	100	100	25-50	1.052
30	62-82	72	82	25-50	1.060
40	40-65	50	65	25-50	1.076
50	23-49	33	49	25-50	1.087
60	11-35	21	35	25-50	1.105
70	2-24	12	24	28-50	1.121
80	0.1-17	7	14	28-50	1.129
90	0.1-14	4	8	28-50	1.136
100	0.1-13	3	5	28-50	1.140
110	0.1-13	3	5	28-50	1.144

Table 5 g-factors (mGy/mGy) for breast thicknesses of 20-110 mm and the HVL range 0.30-0.60 mm Al. The g-factors for breast thicknesses of 20-80 mm are taken from Dance (1990), and for 90-110 mm from Dance et al (2000 & 2011).

Breast thickness (mm)	HVL mm Al										
	0.30	0.35	0.40	0.45	0.50	0.55	0.60	0.65	0.70	0.75	0.80
20	0.390	0.433	0.473	0.509	0.543	0.573	0.587	0.622	0.644	0.663	0.682
30	0.274	0.309	0.342	0.374	0.406	0.437	0.466	0.491	0.514	0.535	0.555
40	0.207	0.235	0.261	0.289	0.318	0.346	0.374	0.399	0.421	0.441	0.460
50	0.164	0.187	0.209	0.232	0.258	0.287	0.310	0.332	0.352	0.371	0.389
60	0.135	0.154	0.172	0.192	0.214	0.236	0.261	0.282	0.300	0.317	0.333
70	0.114	0.130	0.145	0.163	0.177	0.202	0.224	0.244	0.259	0.274	0.289
80	0.098	0.112	0.126	0.140	0.154	0.175	0.195	0.212	0.227	0.241	0.254
90	0.0859	0.0981	0.1106	0.1233	0.1357	0.1543	0.1723	0.1879	0.2017	0.2143	0.2270
100	0.0763	0.0873	0.0986	0.1096	0.1207	0.1375	0.1540	0.1682	0.1809	0.1926	0.2044
110	0.0687	0.0786	0.0887	0.0988	0.1088	0.1240	0.1385	0.1520	0.1638	0.1746	0.1856

Table 6 c-factors for average breasts for women in age group 50 to 64 (Dance et al 2000 & 2011)

Breast thickness (mm)	Gland. %	HVL (mm Al) 0.30	0.35	0.40	0.45	0.50	0.55	0.60	0.65	0.70	0.75	0.80
20	100	0.885	0.891	0.900	0.905	0.910	0.914	0.919	0.923	0.928	0.932	0.936
30	72	0.925	0.929	0.931	0.933	0.937	0.940	0.941	0.947	0.950	0.953	0.956
40	50	1.000	1.000	1.000	1.000	1.000	1.000	1.000	1.000	1.000	1.000	1.000
50	33	1.086	1.082	1.081	1.078	1.075	1.071	1.069	1.064	1.060	1.057	1.053
60	21	1.164	1.160	1.151	1.150	1.144	1.139	1.134	1.124	1.117	1.111	1.103
70	12	1.232	1.225	1.214	1.208	1.204	1.196	1.188	1.176	1.167	1.157	1.147
80	7	1.275	1.265	1.257	1.254	1.247	1.237	1.227	1.213	1.202	1.191	1.179
90	4	1.299	1.292	1.282	1.275	1.270	1.260	1.249	1.236	1.225	1.213	1.200
100	3	1.307	1.298	1.290	1.286	1.283	1.272	1.261	1.248	1.236	1.224	1.211
110	3	1.306	1.301	1.294	1.291	1.283	1.274	1.266	1.251	1.240	1.228	1.215

Table 7 c-factors for average breasts for women in age group 40 to 49 (Dance et al 2000 & 2011)

Breast thickness (mm)	Gland. %	HVL (mm Al) 0.30	0.35	0.40	0.45	0.50	0.55	0.60	0.65	0.70	0.75	0.80
20	100	0.885	0.891	0.900	0.905	0.910	0.914	0.919	0.923	0.928	0.932	0.936
30	82	0.894	0.898	0.903	0.906	0.911	0.915	0.918	0.924	0.928	0.933	0.937
40	65	0.940	0.943	0.945	0.947	0.948	0.952	0.955	0.956	0.959	0.961	0.964
50	49	1.005	1.005	1.005	1.004	1.004	1.004	1.004	1.004	1.003	1.003	1.003
60	35	1.080	1.078	1.074	1.074	1.071	1.068	1.066	1.061	1.058	1.055	1.051
70	24	1.152	1.147	1.141	1.138	1.135	1.130	1.127	1.117	1.111	1.105	1.098
80	14	1.220	1.213	1.206	1.205	1.199	1.190	1.183	1.172	1.163	1.154	1.145
90	8	1.270	1.264	1.254	1.248	1.244	1.235	1.225	1.214	1.204	1.193	1.181
100	5	1.295	1.287	1.279	1.275	1.272	1.262	1.251	1.238	1.227	1.215	1.203
110	5	1.294	1.290	1.283	1.281	1.273	1.264	1.256	1.242	1.232	1.220	1.208

Table 8a t-factors (breast thickness) for the calculation of AGD for individual projections and the full field geometry.

Breast thickness	Conversion factor *t* for Projection angle (degrees)					
(mm)	5	10	15	20	25	30
20	0.997	0.988	0.976	0.958	0.930	0.895
30	0.996	0.986	0.970	0.944	0.914	0.870
40	0.996	0.984	0.964	0.937	0.902	0.859
50	0.995	0.983	0.961	0.932	0.897	0.855
60	0.994	0.980	0.960	0.926	0.894	0.851
70	0.993	0.980	0.956	0.927	0.894	0.851
80	0.993	0.979	0.955	0.924	0.892	0.852
90	0.991	0.977	0.951	0.924	0.892	0.854
100	0.993	0.975	0.949	0.924	0.892	0.845
110	0.992	0.973	0.947	0.921	0.888	0.834

Table 8b t-factors (PMMA thickness) for the calculation of AGD for individual projections and the full field geometry.

PMMA Thickness	Equivalent breast thickness	Conversion factor *t* for projection angle (degrees)					
(mm)	(mm)	5	10	15	20	25	30
20	21	0.997	0.988	0.975	0.956	0.928	0.893
30	32	0.996	0.985	0.968	0.942	0.911	0.868
40	45	0.996	0.984	0.963	0.934	0.900	0.857
45	53	0.995	0.982	0.961	0.930	0.896	0.854
50	60	0.994	0.980	0.960	0.926	0.894	0.851
60	75	0.993	0.980	0.955	0.925	0.893	0.851
70	90	0.991	0.977	0.951	0.924	0.892	0.854
80	103	0.993	0.974	0.948	0.923	0.891	0.842

Table 9a T-factors (breast thickness) for different scan ranges and the full field geometry.

Breast thickness	Conversion factor T for projection angular range of (degrees)				
(mm)	-10 to +10	-15 to +15	-20 to +20	-25 to +25	-30 to +30
20	0.994	0.989	0.982	0.972	0.960
30	0.992	0.985	0.976	0.965	0.950
40	0.992	0.984	0.973	0.961	0.944
50	0.991	0.982	0.971	0.957	0.941
60	0.989	0.981	0.969	0.955	0.939
70	0.989	0.980	0.969	0.955	0.940
80	0.988	0.979	0.967	0.953	0.937
90	0.987	0.977	0.965	0.952	0.937
100	0.987	0.977	0.965	0.952	0.935
110	0.986	0.975	0.963	0.949	0.931

Table 9b T-factors (PMMA thickness) for different scan ranges and the full field geometry.

PMMA thickness	Equivalent breast thickness	Conversion factor T for projection angular range of (degrees)				
(mm)	(mm)	-10 to +10	-15 to +15	-20 to +20	-25 to +25	-30 to +30
20	21	0.993	0.988	0.981	0.971	0.959
30	32	0.992	0.985	0.976	0.964	0.949
40	45	0.992	0.983	0.972	0.959	0.943
45	53	0.991	0.982	0.970	0.956	0.940
50	60	0.989	0.981	0.969	0.955	0.939
60	75	0.989	0.980	0.968	0.954	0.938
70	90	0.987	0.977	0.965	0.952	0.937
80	103	0.987	0.976	0.964	0.951	0.934

Table 10a ***T*-factors (breast thickness) for the following full field tomosynthesis systems (geometry and exposure values as in table 1): Hologic Selenia Dimensions (2011 model), Siemens Mammomat Inspiration tomographic system (2011 model), GE Essential (2013 model), IMS Giotto TOMO (2013 model) and Planmed Nuance Excel DBT (2013 model). Updated versions of Table 10a will be made available on the EUREF website as new equipment becomes available.**

Breast thickness (mm)	$T_{Fujifilm}$ ± 7.5°	$T_{Fujifilm}$ ± 20°	T_{GE} ± 12.5°	$T_{Hologic}$ ± 7.5°	T_{IMS} ± 19°	$T_{Planmed}$ ± 15°	$T_{Siemens}$ ± 24°
20	0.997	0.985	0.993	0.997	0.985	0.991	0.980
30	0.996	0.981	0.991	0.996	0.981	0.989	0.974
40	0.997	0.979	0.990	0.996	0.978	0.988	0.971
50	0.996	0.977	0.989	0.995	0.976	0.986	0.968
60	0.995	0.975	0.988	0.994	0.974	0.985	0.966
70	0.995	0.974	0.987	0.994	0.973	0.984	0.965
80	0.994	0.972	0.986	0.993	0.972	0.983	0.964
90	0.993	0.971	0.985	0.992	0.970	0.981	0.962
100	0.994	0.970	0.984	0.993	0.970	0.981	0.961
110	0.993	0.969	0.984	0.992	0.968	0.980	0.960

Table 10b ***T*$_S$ factors (breast thickness) for the Philips Microdose system with scanning geometry (geometry and exposure values from 2010 prototype). Updated versions of Table 10b will be made available on the EUREF website as new equipment becomes available.**

Breast thickness (mm)	$T_{Philips}$
20	0.983
30	0.958
40	0.935
50	0.907
60	0.883
70	0.859
80	0.833
90	0.806
100	0.783
110	0.759

Table 11a ***T*-factors (PMMA thickness) for the following full field tomosynthesis systems: Hologic Selenia Dimensions (geometry and exposure values for 2011 model), Siemens Mammomat Inspiration tomographic system (geometry and exposure values for 2011 model), GE Essential, IMS Giotto TOMO and Planmed Clarity. Updated versions of Table 11a will be made available on the EUREF website as new equipment becomes available.**

PMMA thickness (mm)	Breast thickness (mm)	$T_{Fujifilm}$ ± 7.5°	$T_{Fujifilm}$ ± 20°	T_{GE} ± 12.5°	$T_{Hologic}$ ± 7.5°	T_{IMS} ± 19°	$T_{Planmed}$ ± 15°	$T_{Siemens}$ ± 24°
20	21	0.997	0.985	0.993	0.997	0.985	0.991	0.979
30	32	0.996	0.980	0.991	0.996	0.980	0.988	0.973
40	45	0.996	0.978	0.990	0.996	0.977	0.987	0.969
45	53	0.995	0.976	0.989	0.995	0.976	0.986	0.968
50	60	0.995	0.975	0.988	0.994	0.974	0.985	0.966
60	75	0.994	0.973	0.987	0.994	0.973	0.984	0.964
70	90	0.993	0.971	0.985	0.992	0.970	0.981	0.962
80	103	0.994	0.969	0.984	0.993	0.969	0.980	0.961

Table 11b ***T*$_S$ factors (PMMA thickness) for the Philips Microdose system with scanning geometry (geometry and exposure values from 2010 prototype). Updated versions of Table 11b will be made available on the EUREF website as new equipment becomes available.**

PMMA thickness (mm)	Breast thickness (mm)	$T_{Philips}$
20	21	0.980
30	32	0.953
40	45	0.921
45	53	0.900
50	60	0.883
60	75	0.846
70	90	0.806
80	103	0.776

Appendix II Noise Power Spectrum (NPS)

Appendix II.1 NPS in the x-y plane

The use of linear system theory metrics on reconstructed planes is under debate. However it is clear that the noise properties of different tomosynthesis systems differ substantially, much more than with current FFDM systems. Therefore an objective measurement of noise seems important. Currently measuring NPS can be performed to ensure stability of the tomosynthesis system and similar settings on several systems of the same type.

Under development:

Method: Select manual exposure mode, typical DBT anode/filter combination and tube voltage, position a 2 mm thick aluminium plate as close as possible to the X-ray tube and set the automatic exposure settings for the attenuation of 2 mm aluminium filter for this breast thickness. Set compression height to 45 mm so that the system reconstructs a volume of 45 mm. Acquire the DBT scan and reconstruct using the standard clinical reconstruction algorithm (this is an air reconstruction with metal (Al) filtration; low scatter). Calculate the NPS from the 20 mm plane using the extraction method of Siewerdsen et al (2002). Use a standard NPS algorithm (50 mm x 50 mm NPS region extracted from centre of x-y plane; detrend by fitting and subtracting 2nd order polynomial from this region; 256 x 256 half-overlapping ROIs; section 0° and 90° axes separately as the in-plane DBT NPS is probably non-isotropic) . Rebin to 0.25 mm^{-1} spatial frequency bins. Record the NNPS at 0.5 mm^{-1} and 2 mm^{-1}.

Remark: This method does not account for / include correlations orthogonal to the direction of extraction. This can underestimate the true NPS if correlations are not accounted for in some way. Correction could be made using a bandwidth integral.

Limiting values: To be determined
Frequency: Every 6 months
Equipment: 2 mm thick aluminium plate

Appendix II.2 NPS in the reconstructed tomosynthesis image

Under development.

Appendix III: Significance of test items

The test-items described in this protocol can be divided in three categories: essential test items which should be measured, desirable test items which are advised to be measured, optional test items which can be measured.

Essential test items:		performed:	
1.4	Tube output	acc.	May be performed in FFDM[1]
1.5.2	HVL	acc.	May be performed in FFDM[1]
1.6	Exposure distribution per projection image	acc./routine	For systems with variable dose per projection
2.1	Back-up timer and security cut-off	acc./routine	
2.2	AEC Short term reproducibility	acc./routine	
2.3	AEC Long term reproducibility	acc./routine	
2.4	AEC performance	acc./routine	
3.1	Compression force	acc./routine	May be performed in FFDM
4.1	Response function and noise analysis	acc./routine	May be performed in FFDM[1]
4.2	Detector element failure	acc./routine	May be performed in FFDM[2]
4.3	Uncorrected defective detector elements	acc./routine	
4.4	System projection MTF	acc./routine	
5.1	Stability of image quality in the x-y plane Image quality test	acc./routine	
5.2	Z-resolution	acc./routine	
5.5	Missed tissue	acc./routine	
5.6	Homogeneity of the reconstructed tomosynthesis image	acc./routine	
5.7	Geometric distortion (full field geometry)	acc.	
6.2.1	Assessing AGD with PMMA	acc./routine	
6.2.2	Assessing clinical breast doses	typetest	
7	Image presentation	acc./routine	
Desirable test items:			
1.2	Focal spot motion	acc./routine	
1.3	Coincidence of reconstructed and irradiated volume	acc./routine	
2.5	Exposure time and total scan time	acc./routine	
2.6	Response to local and global variations in breast density	acc./routine	
4.5	System projection MTF	acc./routine	
5.7	Geometric distortion (scanning geometry)	routine	
6.2.2	Assessing clinical breast doses	acc./routine	
Optional test items:			
1.1	Focal spot size	acc.	
1.5.1	Tube voltage	acc./routine	
1.6	Exposure distribution per projection image	acc.	For systems with equal dose per projection
5.3	MTF in the x-y plane	acc./routine	
5.4	NPS in the x-y plane	acc./routine	

[1] It must be verified whether the target, material and thickness of the filter and readout of the detector is equal in FFDM and DBT mode.
[2] It must be verified whether the readout of the detector is equal in FFDM and DBT mode.

Appendix IV Specifications and tolerances of equipment and phantoms

TableIV.1 Specifications and tolerances of equipment and phantoms.

	Material	Dimensions	thickness	purity
Standard test block	PMMA	At all sides > 5mm larger than X-ray beam	45±0.5 mm	
slabs	PMMA	≥ 240mm x 180 mm	10±0.1mm	
slab	PMMA	≥ 240mm x 180 mm	5±0.1mm	
Z-resolution phantom	PMMA with 25 Aluminium spheres	PMMA: 240.mm x 300.mm	PMMA: 5±0.1 mm Aluminium spheres: 1.00± 0.03 mm	
slabs	High density PE (PE 300)	≥ 240mm x 180 mm	2±0.1 mm 5±0.1 mm 10±0.1mm	
NPS attenuator	Aluminium	Covering the whole X-ray beam	2 mm	99%
MTF phantom	Stainless steel	50 mm x 50 mm	1 mm	
Tungsten wire	Tungsten		25 µm diameter	
SDNR sheet	Aluminium	10±1 mm x 10±1. mm	0.200±0.002 mm	99%
Protective plate	e.g. Stainless steel	covering the whole image receptor	e.g. 3 ± 1 mm stainless steel	
Self developing film	Sensitive for mammography X-ray spectra			
Focal spot size phantom				
CDMAM phantom				
TORMAM phantom				
Block of foam	Density: 30±5 kg/m3, 5.0±1.0 kPa at 40% deformation	240mm x 180mm		
X-ray rulers				

TableIV.2 Specifications of meters.

	Accuracy	Reproducibility
Exposure time meter	5%	1%
Dose meter	5%	1%
Tube voltage meter	5%	1%
Compression force meter	10%	5%

Appendix V List of abbreviations and definitions (provisional)

AEC	Automatic Exposure Control
AGD	Average Glandular Dose
Angle (projection -)	The projection angle is the angle between a line extended from the detector through the object and the normal to the detector.
Angle (tube rotation-	The tube rotation angle is angle between the line connecting 'the center of rotation and the source' and the zero degree line).
Angular range	The difference in the first and last projection angle of a tomosynthesis acquisition.
Bit-depth	Number of values which can be assigned to a single pixel in a specific digital system, expressed in bits.
Centre of rotation	Centre point of the rotational movement of the X-ray tube
DBT	Digital breast tomosynthesis
DBT sequence of images	Full series of images on a DBT system between and including pre-exposure and/or first projection image and the last projection image.
Bad pixel map	A map (either an image or a table) which defines the position of all pixels for which the pixel value is not based on its own del reading (in 2D mammography or projection images in DBT). The maps from 2D and DBT might be different.
Detector binning	0018,701A Detector Binning: 1\1 grouping of individual dels used at the read-out stage 1\1 is no binning; 1\2 is grouping of 2 dels into a single pixel for 1 direction; 2\2 is 4 dels grouped into 1 pixel
Detector corrections	Corrections in DR systems in which the values of defective detector elements/columns/rows are recovered using the detector bad pixel map; additional corrections are also made for variations in individual detector element sensitivity, electronic gain and large area variations in signal (e.g. heel effect, beam divergence).
Del	Single discrete detector element in a DR detector.
Del pitch	(Also referred to as pixel pitch)Physical distance between the centres of adjacent dels. This is DICOM tag (0018;1164) and is called imager pixel spacing. This is generally equal to detector element spacing.
First projection	

image	The first projection image made in a DBT sequence of images with exposure parameters which have been determined by the AEC. Note: This does not have to be the first image in the DBT sequence if a pre-exposure is made in zero degree position.
Ghost signal	Residual signal carried over from previous projection images into successive projection images.
Exposure time	
(projection image)	The duration of the X-ray exposure for a projection image
Exposure time	
(scanning geometry)	The total time between the start and end of the exposure of an individual point of an object in a tomosynthesis sequence.
FFDM	Full Field Digital Mammography, 2D mammography
Focal spot line	Line from the focal spot to the centre of the image receptor
Focal plane	A plane within a reconstructed image in which objects at the height it represents are brought into focus.
Full-field geometry	Geometry of DBT systems incorporating a detector as used in conventional 2D full field digital mammography (FFDM), and an X-ray tube that rotates above this detector. A series of individual projection images, in which the whole breast is irradiated in each exposure, are acquired over a range of angles.
Linearised	
pixel value	In FFDM or tomosynthesis projection images there may not be a directly proportional relationship between pixel value and air kerma at the detector surface. Linearized pixel values are obtained by inverting the system response in which pixel values are plotted against detector air kerma. Following this step, a pixel value measured in an image in which pixel values have been linearized is equal to the detector air kerma. This assumes similar beam qualities for the response curve and the image in question. A linearized image has zero off-set.
Noise	All fluctuations in pixel values except those directly related to the imaged anatomy or structures within a test object. The standard deviation or the variance in a ROI in the image is taken as measure of noise.
Pixel	Picture element, the smallest unit in an electronic image.
Pixel value	Discrete value assigned to a pixel. In mammography systems the number of pixel values range from 1024 (10-bits) to 16384 (14 bits), depending on the system.

Pixel value offset Fixed value that has been added to the values of all pixels during the generation of the projection image. Not all systems have a pixel value offset in the projection images.

PMMA Polymethyl methacrylate

Projection image An image within a series of images, acquired at a specific tube rotation angle. Scanning geometries do not acquire projection images

Processed image The image after image processing, ready for presentation on the monitor or print-out. In the DICOM file the value of the element Presentation Intent Type (0008,0068) is 'FOR PRESENTATION'.

Processed projection image A projection image in which the DICOM tag (0008, 0068) is set to 'FOR PRESENTATION'. A manufacture might process the projection images before image reconstruction.

Raw image See unprocessed image

Reconstructed DBT image Output image of a DBT system consisting of a stack of reconstructed focal planes

Reconstructed focal plane An image representing a particular height within a reconstructed volume, with only objects at that height brought into sharp focus in that focal plane.

Reconstructed volume The volume represented by a reconstructed DBT image**.**

Reference region-of-interest (in the reconstructed plane) A region-of-interest (size:5 x 5 mm) in the plane at 20 mm height above the bucky table in the reconstructed tomosynthesis image. The centre of the region-of-interest is positioned 60 mm perpendicular to the chest wall edge of the table and centred laterally.

Reference region-of-interest (in the projection image) A region-of-interest (size:5 x 5 mm) in the projection image. The centre of the region-of-interest is positioned 60 mm perpendicular to the chest wall edge of the table and centred laterally.

Reference value For some test-items, limiting values are not given. However some guidance is given by the use of reference values, mostly derived from the limiting values in FFDM. These limiting values have been chosen as reference values because the benefit of DBT in e.g. terms of cancer detection and characterization, versus the cost in terms of radiation dose is

not yet clear. Applying too many restrictions in this early stage in the development of DBT may lead to a suboptimal dose-image quality balance. However, exceeding the limiting values of FFDM should only be accepted if clear benefit for the patient/client is expected.

Scan Complete cycle of a tomosynthesis acquisition

Scan Time The time between the start of the first exposure (this could be a test shot in the zero degree postion) and the end of the last exposure of a tomosynthesis sequence.

Scanning geometry Geometry of DBT systems utilising a narrow collimated X-ray beam which scans across the breast as the X-ray tube rotates, and by which the breast is only partially irradiated at each position of the X-ray tube. Due to the design of the system and continuous readout from the detector, individual projection images might not exist.

SDNR Signal Difference to Noise Ratio. If calculated from projection images, these images must first be linearized

$$\mathrm{SDNR} = \frac{PV(signal) - PV(background)}{\mathrm{SD(backgro\,und)}}$$

SNR Signal to Noise Ratio: In FFDM imaging SNR is calculated as follows for a specific ROI. If calculated from projection images, these images must first be linearized

$$\mathrm{SNR} = \frac{\mathrm{PV - PVoffset}}{\mathrm{SD}}$$

Standard test block PMMA test object to represent a typical load for the system. The block may consist of several thinner slabs.

Straight through position The position of the focal spot in which the focal spot line equals the zero degree line.

Threshold contrast The contrast of an object at a given detectability. Detectability can be determined using human or machine scoring.

Unprocessed image A digital image after flat-fielding and detector corrections but before other image processing has been applied. In the DICOM header the value of the element Presentation Intent Type (0008,0068)is ‘FOR PROCESSING’. Sometimes unprocessed images are referred as ‘raw data’

Unprocessed projection image A projection image without processing. See defintions of unprocessed image and projection image

Variation $\frac{\min - \max}{mean}$ x 100%

Z-direction On DBT systems, the z-direction is perpendicular to the reconstructed planes.

Zero degree projection A projection in which a line through the focal spot and centre of rotation is perpendicular to the bucky surface.

Zero degree angle stationary mode A stationary mode at zero degree angle which produces projection images in which the exposures of all projection images is given without movement of the X-ray tube. In this mode it must be possible to choose similar X-ray spectra as in standard DBT mode. AEC should be working as for a moving tube DBT scan. Projection images should have the same corrections (e.g. gain, flat fielding, etc.) as for the moving tube DBT scan.

Zero degree line A line from the focal spot towards the centre of rotation so that the focal spot line is perpendicular to the bucky surface.

Zero degree line (line connecting the center of the rotation and the source when the tube is in the nominal 0° position)